NAVAL POSTGRADUATE SCHOOL
Monterey, California

THESIS

MODELING A RAIN-INDUCED MIXED LAYER

by

Hur, Hong Beom

June 1990

Thesis Advisor Jeffrey A. Nystuen

Unclassified

security classification of this page

REPORT DOCUMENTATION PAGE

1a Report Security Classification: Unclassified			1b Restrictive Markings
2a Security Classification Authority			3 Distribution/Availability of Report: Approved for public release; distribution is unlimited.
2b Declassification/Downgrading Schedule			
4 Performing Organization Report Number(s)			5 Monitoring Organization Report Number(s)
6a Name of Performing Organization: Naval Postgraduate School	6b Office Symbol (*If applicable*) 35		7a Name of Monitoring Organization: Naval Postgraduate School
6c Address (*city, state, and ZIP code*): Monterey, CA 93943-5000			7b Address (*city, state, and ZIP code*): Monterey, CA 93943-5000
8a Name of Funding/Sponsoring Organization	8b Office Symbol (*If applicable*)		9 Procurement Instrument Identification Number
8c Address (*city, state, and ZIP code*)			10 Source of Funding Numbers: Program Element No / Project No / Task No / Work Unit Accession No

11 Title (*Include security classification*): MODELING A RAIN-INDUCED MIXED LAYER

12 Personal Author(s): Hur, Hong Beom

13a Type of Report	13b Time Covered From To	14 Date of Report (*year, month, day*)	15 Page Count
Master's Thesis		June 1990	65

16 Supplementary Notation: The views expressed in this thesis are those of the author and do not reflect the official policy or position of the Department of Defense or the U.S. Government.

17 Cosati Codes			18 Subject Terms (*continue on reverse if necessary and identify by block number*)
Field	Group	Subgroup	

19 Abstract (*continue on reverse if necessary and identify by block number*)

With the development of ocean surface remote sensing, air-sea interaction theory and the theory of underwater sound generation at the ocean surface, the potential calming effect on surface gravity waves by raindrop induced mixing has become important. The rain induced mixed layer was studied with models based on the turbulent kinetic energy budget. A bulk mixed layer model proposed by Garwood was tuned with laboratory experimental data from Green and Houk (J. Fluid Mech., 1979). The turbulent kinetic energy going into subsurface mixing was found to be less than 10% of the total raindrop kinetic energy. The length scale for mixing is proportional to both raindrop size and rain intensity. Furthermore, there is some indication of an initial penetration depth for raindrops. Although the available data was inadequate to complete model development and verification, a prediction for a hypothetical situation in the North Pacific is proposed. The diffusion processes are illustrated by solving for the diffusion and dissipation terms of the turbulent kinetic energy equation with a finite difference scheme. New experiments are suggested to allow future model development and testing.

20 Distribution/Availability of Abstract	21 Abstract Security Classification	
☒ unclassified unlimited ☐ same as report ☐ DTIC users	Unclassified	
22a Name of Responsible Individual: Jeffrey A. Nystuen	22b Telephone (*include Area code*): 418-646-2917	22c Office Symbol: 68Oc

DD FORM 1473,84 MAR — 83 APR edition may be used until exhausted. All other editions are obsolete — security classification of this page

Unclassified

ABSTRACT

With the development of ocean surface remote sensing, air-sea interaction theory and the theory of underwater sound generation at the ocean surface, the potential calming effect on surface gravity waves by raindrop induced mixing has become important. The rain induced mixed layer was studied with models based on the turbulent kinetic energy budget. A bulk mixed layer model proposed by Garwood was tuned with laboratory experimental data from Green and Houk (J. Fluid Mech., 1979). The turbulent kinetic energy going into subsurface mixing was found to be less than 10% of the total raindrop kinetic energy. The length scale for mixing is proportional to both raindrop size and rain intensity. Furthermore, there is some indication of an initial penetration depth for raindrops. Although the available data was inadequate to complete model development and verification, a prediction for a hypothetical situation in the North Pacific is proposed. The diffusion processes are illustrated by solving for the diffusion and dissipation terms of the turbulent kinetic energy equation with a finite difference scheme. New experiments are suggested to allow future model development and testing.

TABLE OF CONTENTS

LIST OF TABLES

LIST OF FIGURES

I. INTRODUCTION

The kinetic energy of raindrops at the sea surface can potentially play a role in near surface turbulent mixing. Such mixing will have an effect on satellite remote sensing, air-sea interaction, wave energy propagation and underwater ambient noise production through the reduction of surface gravity waves, temperature changes due to dilution, and bubble creation. Recognizing this importance of rain mixing, it may be useful to create a model which can predict the turbulent upper layer induced by raindrops. The results might indicate the surface gravity wave damping rate which might be used to correct satellite data. As an initial step a model was built to investigate turbulent layer behavior.

The energy of raindrops can go into surface ripples (Poon et al. 1989), subsurface turbulent mixing (Chapman and Critchlow 1967; Siscoe and Levin 1971), and sound (Medwin et al. 1990), although the partition of energy to ripples and mixing is not yet clear. In early studies about water droplets, the energy available for mixing has been closely related to surface configuration and to drop shapes. When a water drop hits the down slope or trough of an existing surface wave (absorption effect), the drop energy goes mainly into surface ripples. On the other hand, when the point of initial contact is upslope or at the crest of a wave (reflection effect), there is a high Rayleigh jet, and most of the energy goes to subsurface mixing (Siscoe and Levin 1971). Keedy (1967) shows that the water drop changes its form from spherical to vertically obliated and prolated while it falls. If the impact occurs when the drop is in a vertically obliated form, the energy available for subsurface mixing is much larger than for the case of collision while in a prolated form. These earlier observations indic. ⁼ that some energy goes into surface waves, some of it goes into subsurface mixing, and the rest of it goes to minor effects, e.g. sound generation.

Assuming that some energy does go to mixing, Nystuen (1990) proposed e-folding times for surface gravity wave attenuation for various pairs of rain induced turbulent layer depth and eddy viscosities (Fig. 1). The most realistic values of eddy viscosity for these predictions were not known. These results show that the strong mixing in a thin turbulent layer will rapidly damp short, less than one meter wavelength, gravity waves. In high wind conditions (larger background eddy viscosity; curves G and H) the increased attenuation is important only for short wavelengths. The short gravity waves

influencing SAR, scatterometer, altimeter and passive radiometers will be damped if substantial energy goes into mixing.

Subsurface mixing by rain on a calm surface was investigated experimentally by Green and Houk (1979) using uniform water drops or a combination of various drop sizes to simulate real rain. The integrated effects of Rayleigh jets, vortex rings and surface gravity waves were assumed to influence entrainment and mixed layer depth. The experiments show that the molecular effects are small compared with the mechanical mixing (inertial effects) due to the rain. The resulting mixed layer depth profiles suggested that the drop size has a major effect on mixing and that the intensity of rainfall is also important. Most of the experiments were done on fresh water for five combinations of drop sizes: fine spray where all of the drop had diameters less than 1.5 mm, rain with uniform drop sizes of 2.2, 3.6 and 5.5 mm diameter respectively, and also with a mixture of the above drop sizes. Mixed layer depth after a fixed time interval was proportional to rain intensity and total kinetic energy. For larger drop sizes, the mixing was more vigorous. Entrainment velocity was defined by the rate that the mixed layer deepened with time. This was inversely proportional to the bulk Richardson number. In salty water trials, mixing is less active due to the strong buoyancy damping from the salinity induced density difference between the fresh water rain and the salty water.

In this thesis, these phenomena are studied with models. Two kinds of models were tried. The bulk mixed layer model, originated by Kraus and Turner (1967), is spatially one dimensional (time and depth) and considers the integrated turbulent kinetic energy in the mixed layer, assumed to be fully turbulent. After Kraus and Turner (1967), a large number of bulk models have been proposed. These models were designed to simulate wind mixing rather than rain mixing. Garwood (1977) presented an advanced bulk mixed layer model having two original points. One is the fraction of wind-generated turbulent kinetic energy partitioned to potential energy. This is increased by means of mixed layer deepening, which is dependent upon layer stability. The other is that viscous dissipation is enhanced for increased values of the reciprocal of Reynolds number. These models are based on the turbulent kinetic energy (TKE) equation derived from the Navior-Stokes equation. Garwood (1990) built a rain mixing model by rewriting the NPS bulk mixed layer model, adjusting to the case of rain mixing. Since real world data is almost non-existent for this problem, the experimental data of Green and Houk was used to tune this model. There were four tuning constants which resulted in an undetermined problem which will be discussed in more detail.

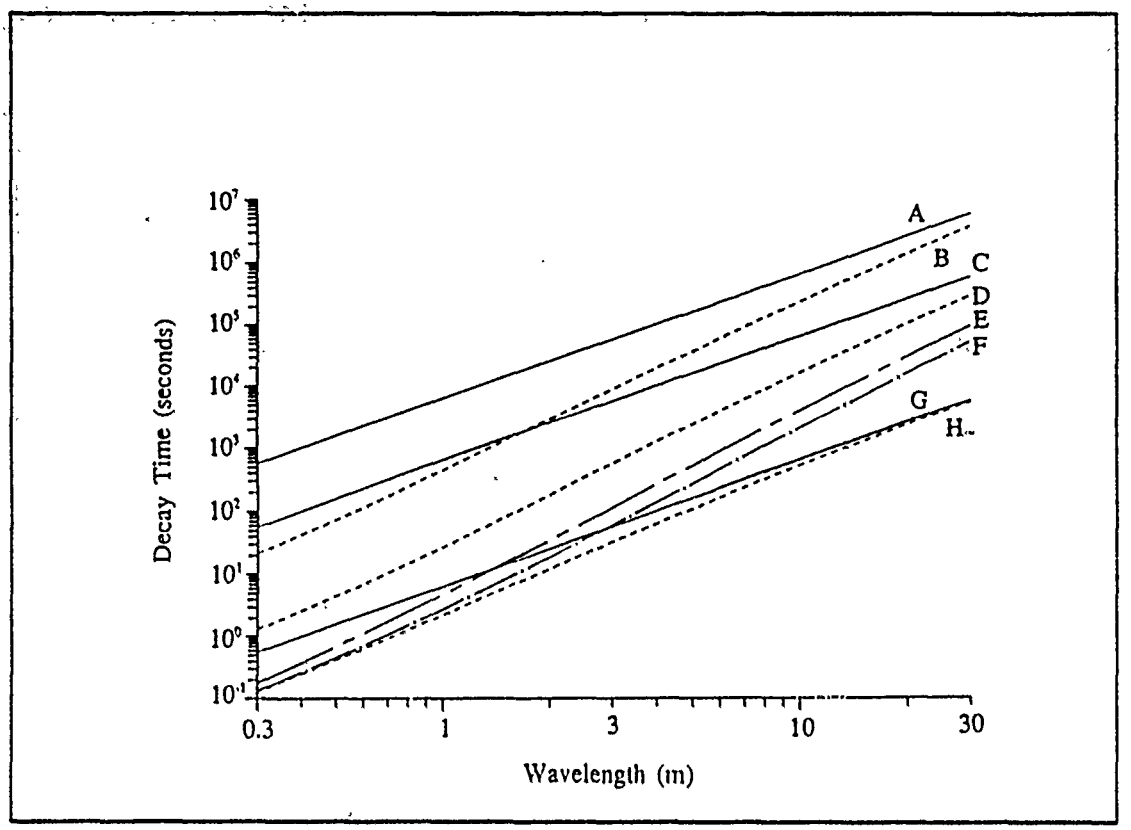

Figure 1. The e-folding Times for Surface Gravity Wave Attenuation as a function of wavelength for several choices of background eddy viscosity, rain-induced turbulent layer viscosity and turbulent layer thickness. Curve A shows the attenuation rate due to molecular mixing. Curve B shows the decrease in decay time (increased attenuation rates) when a layer of weak mixing is present. Curves C - F are for light wind conditions where the background eddy viscosity is assumed to be $10^{-5} m^2/s$. Curve C has no turbulent layer; Curve D has moderate mixing; Curves E and F have strong rain-induced mixing. Curves G and H show the much smaller influence of a rain-induced turbulent layer in moderate wind conditions when the back ground eddy viscosity is larger. Curve G is for the case of no rain and Curve H has a 0.1 m turbulent layer.

Another type of model is a diffusion model which encodes the diffusion and dissipation terms of the TKE equation using a finite difference scheme. This type of model tries to have the turbulence energy propagate itself to deepen the mixed layer. Because

of stability problems for the non-steady solution, we only used it to show the fine structure within the mixed layer after first using the bulk mixed layer model to predict the mixed layer depth.

The main emphasis for this paper is to estimate the best tuning constant values for the rain model. This process will be described in Chapter 3 with a discussion of the significance of the chosen values in Chapter 4. One pair of optimum values will be applied to an hypothetical ocean situation to provide a prediction for mixed layer formation by rain.

II. EXPERIMENTAL EVIDENCE

A. EXPERIMENTAL SETUP OF GREEN AND HOUK

The experimental setup of Green and Houk (1979) is represented in Figure 2. Rain modules, water-filled boxes with holes in the bottom, were used to generate the artificial rain. The rain intensity was varied by changing the water head in the module. Each module was 15 cm deep and 64.5 cm square. Modules were constructed to produce artificial rain with uniform drop sizes (3 different drop diameters) and to approximate natural rain with intensities of about 1.25 cm/h (2% of 5.5 mm, 13% of 3.6 mm, 85% of 2.2 mm drops) and 2.5 cm/h (4% of 5.5 mm, 23% of 3.6 mm, 73% of 2.2 mm drops). The experiment took place in a vertical shaft with dimensions of $3 \times 6 \times 16$ m. The rain module was placed 14 m above the receiving tank. The tank bottom and three of the walls were made of $\frac{3}{4}$ in. marine plywood. The fourth wall was made of $\frac{1}{4}$ in. glass. One inch of styrofoam insulation was placed on the inside walls and bottom.

The temperature was measured by thermopiles (22 vertically aligned in the tank) and sampled every 14.4 s with the accuracy of $\pm 0.05^{\circ}C$. A Fenwall thermistor, mounted on a vertical rod (designed to move up or down with velocity of 1.1 cm/s) was also used to get the vertical temperature profile with the same accuracy. The skin temperature (top $10 \sim 100\ \mu m$) was measured by a radiation thermometer. Because the temperature of rain falling through a deep layer of air will reach and remain at the air wet-bulb temperature, the rain module was kept to within $0.25^{\circ}C$ of the wet-bulb temperature by a Haake FK2 constant temperature bath. The rain drops were generated using hypodermic needles to generate known drop sizes with diameters of 2.2, 3.6 and 5.5 mm. The drop sizes were calibrated placing five drops into a previously weighed beaker of olive oil. The rain intensity was determined by measuring the surface height using a plastic ruler and a low-pass capacitance wave gauge. In the salty receiving tank, the rain intensity was measured by ruler only, and the conductivity gauge was used on the moving probe, instead of the thermistor, to measure salinity. The receiving tank was left undisturbed for 20 minutes prior to the start of each experiment. The tank water temperature was adjusted with ice prior to beginning the experiment. A plastic sheet was placed underneath the module before each experiment, and was removed to start the experiment.

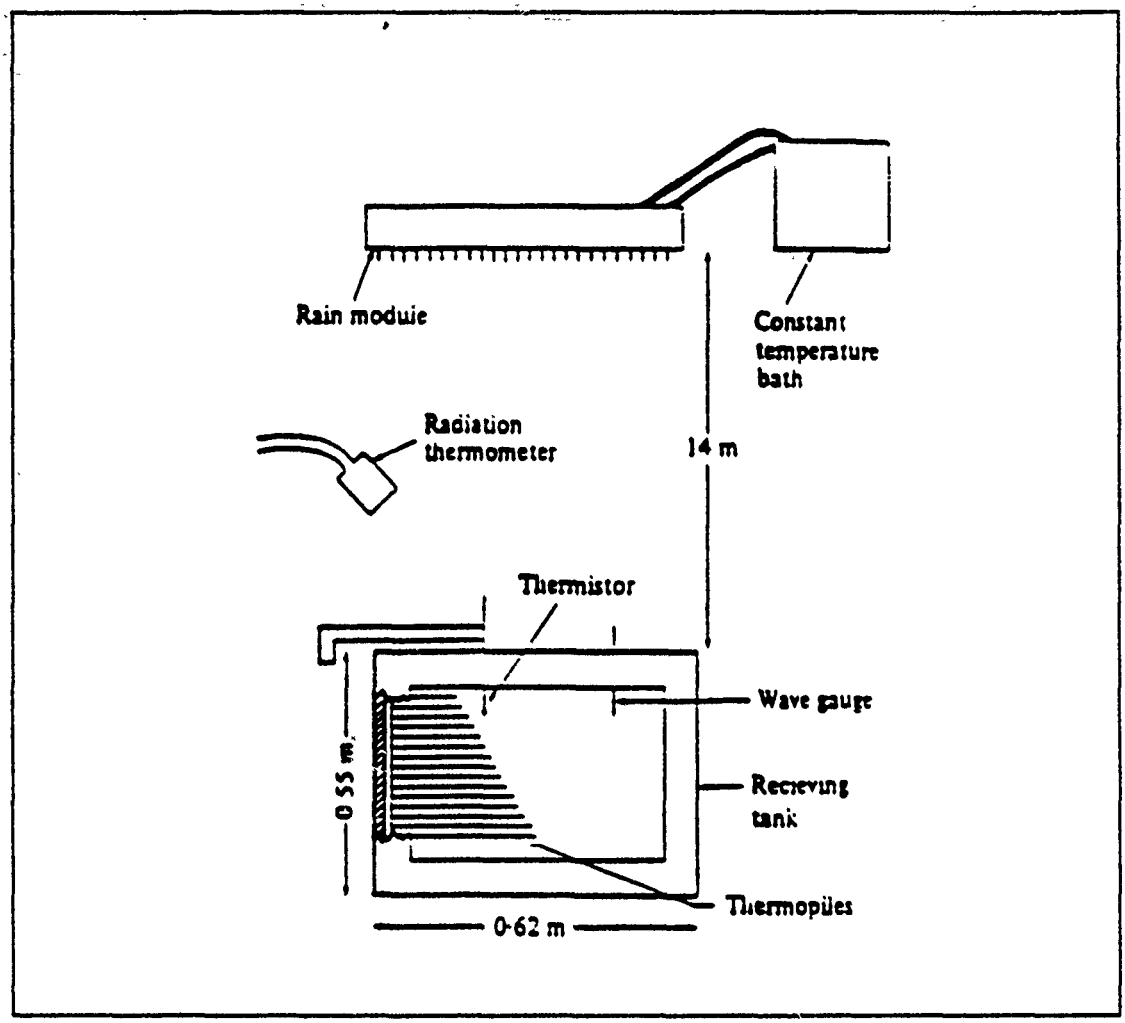

Figure 2. A Schematic Diagram for the Experimental Setup of Green and Houk.

Table 1 presents the rain and environmental conditions for the experiments reported by Green and Houk (1979). The temperature of rain is higher than that of the water surface in most cases; i.e., special attention was paid to the case of warm rain falling on colder fresh water. The impact of water drops creates a turbulent mixed layer which gradually deepens with time, mainly through the entrainment of the fairly quiescent fluid below the mixed layer. Internal waves exist at the thermocline (the lower boundary of the mixed layer) and capillary-gravity waves were on the surface. The surface was disfigured by Rayleigh jets and by many bursting bubbles or secondary splashes associated with the rain drop impacts. Vortex rings are also present, and it is unclear how they, or the waves, interact with the mixed layer turbulence. Green and Houk studied the

integrated effects of all of these phenomena, and dealt with these effects in terms of entrainment and mixed layer depth (Green and Houk 1979).

Table 1. CONDITIONS FOR THE FRESH WATER RAIN EXPERIMENT. All temperature are in °C

Drop size (mm)	Intensity (cm/h)	Air temperature	Air wet-bulb temperature	Initial surface water temperature	Bottom water temperature
≤ 1·6	0·40	23·1	16·7	9·75	6·25
	0·50	23·1	16·7	8·75	6·40
	0·80	23·1	16·7	9·10	6·60
	0·90	23·1	16·7	15·30	13·90
	0·35	23·7	16·5	15·30	13·70
	0·90	23·7	16·5	15·35	13·90
	0·60	23·7	16·5	21·15	21·90
	0·50	23·7	16 5	19·30	19·90
2·2	0·60	22·7	16·5	8·95	6·15
	1·20	22·7	16·5	8·90	6·50
	1·80	22·7	16·3	9·00	6·18
	1·80	22·7	16·3	12·40	10·60
	1·10	23·0	15·5	11·40	10·00
	1·45	24·0	15·7	11·85	10·20
	1·40	24·0	15·8	12·50	10·80
	1·10	24·0	15·8	10·15	8·95
	0·50	23·9	18·0	16·40	15·40
	1·60	25·0	17·8	16·10	15·30
	0·20	25·0	17·8	18·90	19·10
	1·20	25·0	17·8	18·95	19·15
3·6	0·30	23·5	15·0	7·60	6·35
	1·45	23·9	17·5	13·25	11·25
	2·45	23·9	17·5	12·95	11·40
	3·45	23·9	17·5	13·35	11·50
	2·20	23·3	16·7	8·95	6·25
	1·60	23·3	16·7	8·05	6·60
	3·70	23·3	16·7	9·30	6·60
	1·85	23·2	17·2	15·80	14·35
	3·50	24·3	17·8	19·70	20 00
	2·90	24·3	17·8	21·50	21·85
5·5	0·70	23·5	16·7	9·40	6 20
	1·20	23·8	17·0	9 30	6 20
	2·30	23·8	17·0	9·50	6·60
	2·20	23·8	17·0	12·70	11·45
	0·40	23·3	16·0	12·00	10·75
	1·10	23·3	16·0	12·85	10·50
	1·15	23·3	16·0	13·00	10 75
	1·40	23·3	16·0	15·10	13·55
	0·30	22·8	15·0	14·40	12·70
	2·10	22·8	15·5	16·95	17·60
	0·90	22·8	15·5	16·90	17·45
Variable	1·20	23·9	17·4	10·25	6·85
	1·30	23·9	17·4	13·75	11·40
	1·40	23·9	17·4	16·45	15·40
	1·40	23·9	17·4	19·00	19 50
	2·00	23·9	17·5	21·10	21·60
	2·10	23·9	17·5	12·50	7·65
	2·55	23·9	17·5	13·10	11·85
	2·40	23·9	17·5	15·95	14·35

B. DISCUSSION

It is known that some of the raindrop energy may go into subsurface motions not associated with surface waves (Chapman and Critchlow 1967). Siscoe and Levin (1971) investigated the splashes that occur in the presence of surface waves experimentally. They found there are two modes; one produces almost no Rayleigh jets, but strong surface waves, and the other produces unusually high Rayleigh jets, but less strong surface waves. The first mode was defined to be an "absorption" event which occurs when the drop hits the trough, or the down slope of a surface wave. The latter is called a "reflection" event, and occurs when the drop hits the crest or the upslope of a surface wave. Very little kinetic energy goes into the jet in an absorption event, whereas considerable kinetic energy goes into the jet in a reflection event (Siscoe and Levin 1971).

A subsurface vortex ring, produced by rain drops, derives its energy mainly from the surface energy of the drops. There are two conditions for optimum vortex ring formation: the drop must be spherical or it must be changing from an vertically oblated to prolate spheroid upon contact with the receiving tank water (Chapman and Critchlow 1967). Keedy (1967) showed that the penetration of the rings is related to the initial circulation in the drop and the density difference of the rain and receiving water. In general, with larger circulation or smaller density difference, there is greater penetration. The characteristics of the ring are highly dependent on the shape of the drop when it hits the surface. In the case of equal density of the drop and the receiving water, the ring diameter increases linearly with penetration to within about a ring diameter of the critical depth. The critical depth is the depth where the rings stop (rain onto salty water), or transforms into several smaller rings of very low velocity (on fresh water). For the salty water case, the ring diameter increases linearly with penetration for a time, but then assumes a constant size or even decreases with continued penetration. This suggests that rainfall on salty water will not generate as a deep a turbulent layer as rainfall on fresh water.

Figure 3 shows several vertical temperature profiles obtained by Green and Houk. The profiles qualitatively show that mixed layer depth is closely related to the drop size and rain intensity. The initial temperature profiles show that the water within 6 cm of the surface is slightly warmer than the underlying water. This shows that, before the rain starts, the sensible heat flux from the air and the net long-wave radiation flux due to the warm shaft walls more than balances the cooling effect of evaporation at the surface. This profile can be expected in the real world where a calm water surface condition exists. Once rain drops start falling, mixing disrupts this initial condition.

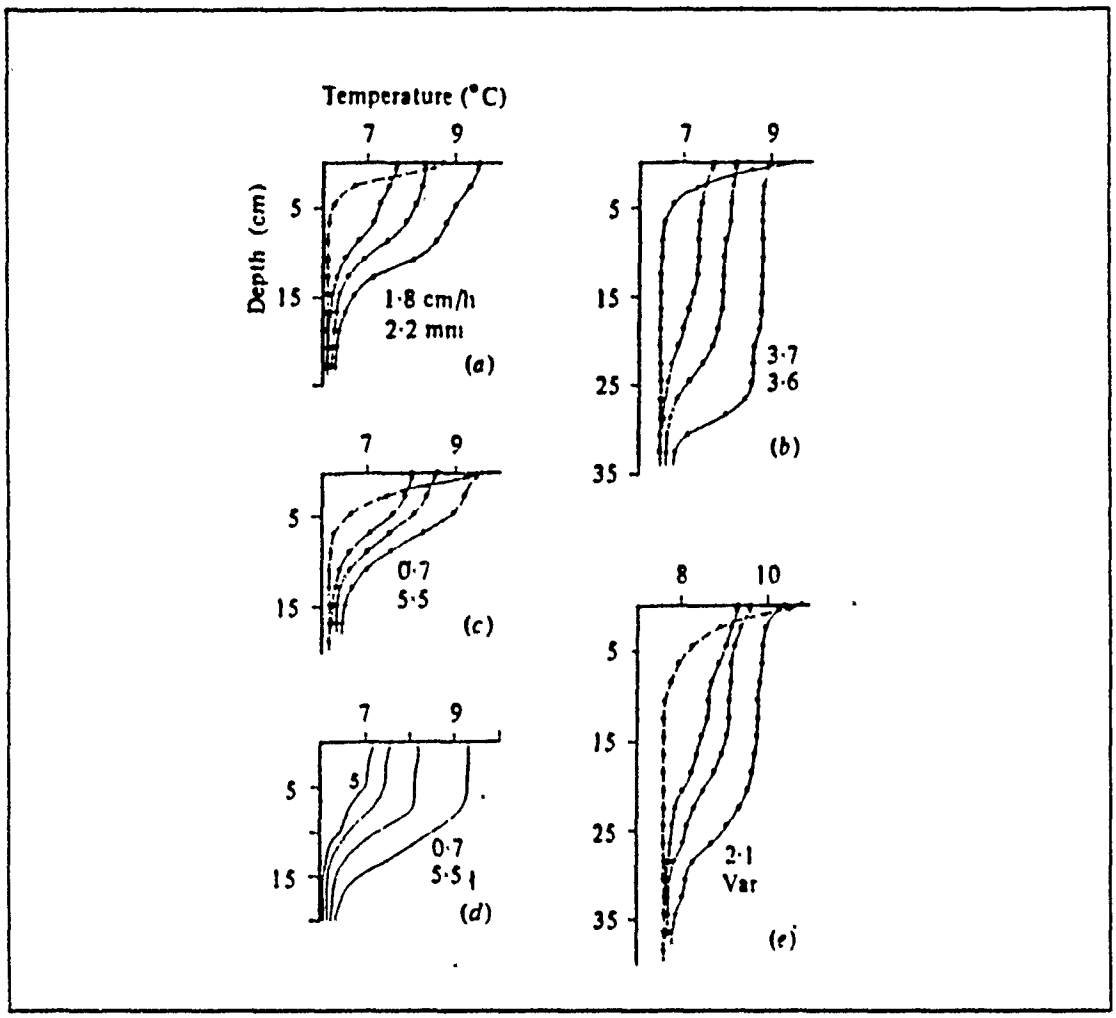

Figure 3. Representative Temperature Profiles of Green & Houk's Experiment. (a),(b),(c),(e) show thermocouple profiles at t = 0, 15, 30, 60 min; (d) shows thermistor profiles at t = 5, 15, 30, 60 min. The rain intensity (upper number) and drop size appear on each figure. The heat stored near the surface always increases with time.

Typical sizes of rain drops are from 0.5 mm to 5.5 mm in diameter (Marshall and Palmer 1948). Figure 4 shows the relation between raindrop diameter (D), the number of drops per unit volume (N_D) and the rain intensity (R). N_D depends on the drop size and rain intensity. The drop sizes and rain intensities used in Green and Houk's experiments are in Table 1. The most commonly discussed conditions in this thesis have in-

tensities of 0.6 cm/h for 2.2 mm drops, 1.6 and 3.7 cm/h for 3.6 mm drops and 2.3 cm/h for 5.5 mm drops.

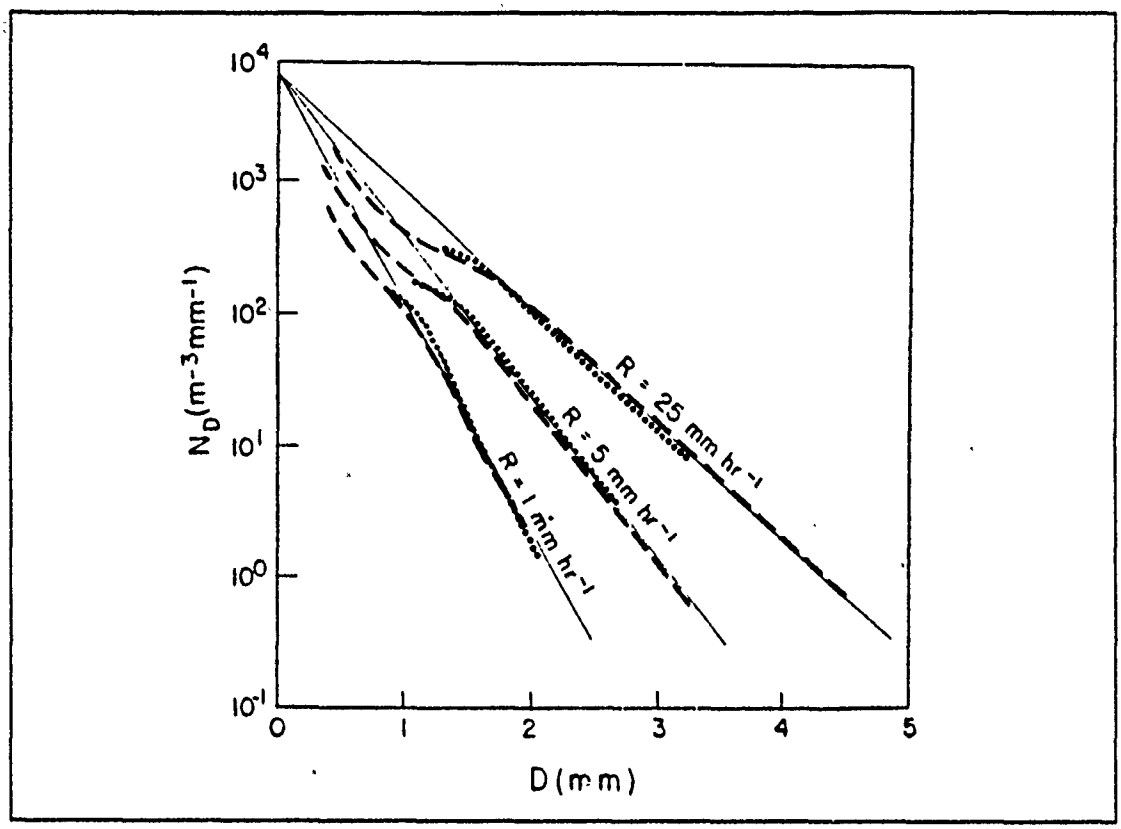

Figure 4. Typical Rain Drop Sizes.

The maximum vertical temperature gradient increases with both increasing mixed layer depth and time due to the heat added to the upper layer, and the relatively small effect of molecular heat diffusion near the surface. The mixing by the larger drops was clearly more vigorous than that from the smaller drops.

The mixed layer depth (H) was defined two ways. One definition is to use the mid-point of the depth interval over which the maximum temperature gradient occurred (this definition tends to remove the effect of molecular heat conduction). The other is the level above which 90 % of the heat transferred through the surface is stored. Table 2 compares the mixed layer depth calculated for each of the above two definitions. The mixed layer depth varies little whether calculated using the heat storage definition or the midpoint of temperature gradient maximum definition. This suggests that the molecular effects are small compared with the mechanical mixing by the rain.

Table 2. COMPARISON OF MIXED LAYER DEPTHS (IN CM) Calculated from the heat storage (Dh) and from the maximum temperature gradient (Dt).

Drop size (mm)	Intensity (cm/h)	Dt (10 min)	Dh (10 min)	Dt (40 min)	Dh (40 min)
2.2	0.6	5.7	6.2	7.2	8.4
	1.80	8.0	8.5	11.0	11.2
	1.80	8.2	8.9	11.0	10.6
3.6	1.60	10.5	11.7	14.8	16.7
	3.70	15.3	15.3	25.0	24.7
	0.3	5.0	7.7	7.8	10.2
5.5	0.40	5.5	5.7	8.9	9.8
	1.2	13.5	13.9	27.0	27.5
	2.30	28.0	25.6	38.5	37.4
Variable	1.30	10.1	11.3	16.2	16.7
	2.10	19.7	18.8	26.0	25.5

Figure 5 shows the mixed layer depth after 20 min of rainfall into both fresh and salt water. This clearly shows the effects of drop size and intensity. The effects of large drops are especially evident in experiments in which variable drop sizes were used. Even if there are only a few large drops, the mixed layer depth is larger than for higher intensity rain experiments which contained only smaller drops. The mixed layer depth should be strongly affected by the mechanical energy flux through the water surface; $\Phi = \rho u_*^3 = \frac{1}{2} \rho \times I \times (terminal\ velocity)^2$ where I is the rain intensity, ρ is the density of a rain drop, u_* is the arbitrary velocity scale used in the turbulence layer following the guidelines of Green and Houk, and Φ is the kinetic energy flux at the surface (J/m^2s).

Green and Houk defined the descent of the thermocline due to the upward entrainment of the lower fluid by an entrainment coefficient E. This coefficient is defined as the ratio of the descent rate $\frac{dH}{dt}$ to a characteristic velocity in the turbulent layer (u_*), i.e., $E = \frac{dH}{dt} u_*^{-1}$. The entrainment coefficient (E) is a function of the bulk Richardson number, which is defined as $Ri = \frac{gH\Delta\rho}{\rho u_*^2}$. The entrainment coefficient was inversely proportional to the Richardson number (slope is -1 for each drop size) regardless of the drop sizes present in the rain.

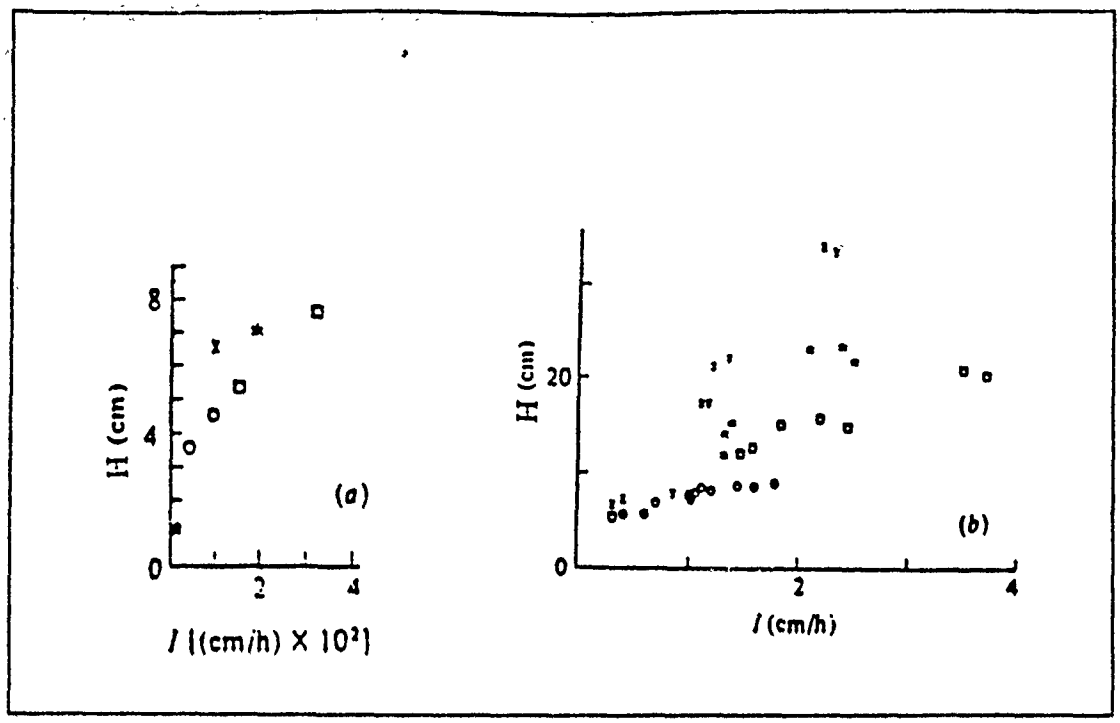

Figure 5. Mixed Layer Depth After 20 Minutes of Rain. I is the rain intensity in cm and H is the mixed layer depth. The empty circle symbol is for rain with 2.2 mm drops, the empty box is 3.6 mm drops, 'x' represents rain with 5.5 mm drops and '*' is for rain with variable drop sizes.

As a summary, the Green and Houk experiments prove that larger rain drops produce deeper mixed layers and suggest that a deeper mixed layer is generated in a fresh water body than that of a corresponding salt water body. The entrainment coefficient is inversely proportional to the bulk Richardson number.

III. MIXED LAYER MODELING

A. INTRODUCTION TO MODEL TYPES

1. The NPS Bulk Mixed Layer Model

The bulk mixed layer model is an one dimensional model. Typically, a fully turbulent mixed layer is assumed to be bounded above by the air-sea interface and below by a dynamically stable water mass. There is a sharp density jump between this upper layer and the water below. This density jump provides the conditions for Kelvin-Helmholtz instabilities at the interface. This region, which is intermittently turbulent in comparison with the overlying mixed layer, is called the 'entrainment zone'. An entrainment velocity usually is defined as the rate of increase of mixed layer depth (MLD).

For a rain-induced mixed layer, the kinetic energy for generating the turbulence comes from the kinetic energy of the falling raindrops. It is assumed that there are enough raindrops to maintain the turbulence in the upper layer and to deepen it. Even if a large drop penetrates to a certain depth, the mixed layer produced by that drop cannot be maintained due to dissipation and buoyancy damping. If raindrops are sparse enough, the turbulence will disappear in a few seconds and the upper layer of water will stay in a laminar state.

As the kinetic energy is transported from the surface to the entrainment zone, some energy is lost to dissipation. This loss was neglected in the prototype one-dimensional model of Kraus and Turner. Subsequent studies showed that this dissipation term is important.

The concepts described above were modeled using the turbulent kinetic energy (TKE) equation, vertically integrated across the mixed layer. The TKE equation for typical wind mixing is,

$$\frac{\partial}{\partial t}\left(\frac{\overline{E}}{2}\right) = -\left[\overline{u'w'}\frac{\partial \overline{u}}{\partial z}\right] - \frac{\overline{w'\rho'}}{\rho_0}g - \frac{\partial}{\partial z}\overline{\left[w'\left(E+\frac{p'}{\rho_0}\right)\right]} - \varepsilon \qquad (1)$$

(A) (B) (C) (D)

where, $E = \overline{u'^2}+\overline{v'^2}+\overline{w'^2}$, u,v and w represent the velocity component of the upper layer, ρ is density and g is gravity. The prime indicates the perturbation term while subscript

zero and overbar indicate mean quantities. Term (A) represents shear production from wind forcing, (B) is the buoyancy flux, (C) is the TKE transport term and (D) is the dissipation term. The wind stress source term (term (A)) does not exist in rain mixing and raindrop kinetic energy flux, the (C) term evaluated at surface after vertical integration, takes the role of the source term. In the NPS rain induced bulk mixed layer model, hereafter referred to as the NPS bulk rain model, or more briefly, as the rain model, the mixed layer is assumed to be fully turbulent as in the other bulk models. In the following discussion, the vertically integrated form of each term of equation (1) will come up.

2. Diffusion Model

This type of model is radically different from the NPS bulk model in the sense that it attempts to have the kinetic energy of the turbulence diffuse itself downward. Unlike the NPS bulk model, there is no vertical integration over the mixed layer depth. Earlier attempts with this type of model have had difficulty predicting the growth of wind-driven mixed layers (Garwood 1990). Because of the difficulty in using this model to predict the growth of the mixed layer, we attempted to use it to investigate potential steady state solutions. The purpose of this model became mainly to show the kinetic energy profile of the NPS bulk rain model more realistically.

The reduced turbulent kinetic energy equation is,

$$\frac{\partial \rho k}{\partial t} + \frac{\partial \rho k u_k}{\partial x_k} = a_k \frac{\partial p}{\partial x_k} - R_{ik} \frac{\partial u_i}{\partial x_k} + \frac{\partial}{\partial x_k}(\rho \nu_t \frac{\partial k}{\partial x_k}) - \rho \varepsilon.$$

When we assume that there are no mean velocities and no horizontal gradients, the equation becomes,

$$\frac{\partial \rho k}{\partial t} = a_k \frac{\partial p}{\partial z} + \frac{\partial}{\partial z}(\rho \nu_t \frac{\partial k}{\partial z}) - \rho \varepsilon$$

i.e., the buoyancy, diffusion and dissipation terms remain. As a first approach to modeling the TKE equation, the buoyancy term was neglected,

$$\frac{\partial k}{\partial t} = \frac{\partial}{\partial z}(\nu_t \frac{\partial k}{\partial z}) - \varepsilon \qquad (2)$$

where the viscosity was $\nu_t = D\sqrt{k}$, dissipation was $\varepsilon = \frac{k^{\frac{3}{2}}}{D}$, and D was the mixing length scale.

For the stability analysis, the direct method, energy method or the von Neuman method are usually used. The direct method investigates the ratio of k^{n+1} and k^n directly and the criterion is that the ratio is less than 1. The energy method tests whether the sum of squares, $\sum_j (k_j^n)^2$, is bounded or not. It assumes cyclic continuity. The von Neuman method assumes that the solution has a wave form, substitutes this solution into the finite difference equation and examines the behavior of the amplitude of k^n for each wave number m. This has to be stable for all m to be genuinely stable. For this problem, the diffusion equation is non-linear. For non-linear cases, the energy method usually works best, but cyclic continuity does not hold for this situation. Thus, for simplicity, the von Neuman method was chosen for this problem.

3. Combining the Models

The NPS bulk rain model can be used to determine the MLD for various rain mixing situations, but it does not attempt to model the structure within the mixed layer (i.e. it is vertically integrated). The diffusion model explicitly models the diffusion of TKE coming through the surface down to the mixed layer depth. It works best with a steady state situation and does not predict the MLD very well. Given these two reasons, we attempted to combine the two models to produce a more realistic TKE profile within the mixed layer.

Combining these two types of model do not include unifying the codes themselves. The bulk rain model was run first, and for any particular time, the values of TKE and MLD can be determined. These two pieces of information become the input to the diffusion model. The assumption of the NPS bulk model that there is no TKE below the entrainment zone is maintained.

B. DIFFUSION MODEL EFFORT

1. Development

The modeling effort for equation (2) uses a finite difference scheme. There are many different time differencing schemes. A list of some of the most basic and frequently used schemes are in Table 3.

As a first approach, we considered only the diffusion and dissipation terms in a steady state situation.

Equation (2) can be scripted as follows,

$$\frac{\partial k}{\partial z} = \frac{1}{2} Dk^{-\frac{1}{2}} \left(\frac{\partial k}{\partial z}\right)^2 + Dk^{\frac{1}{2}} \frac{\partial^2 k}{\partial z^2} - \frac{k^{\frac{3}{2}}}{D}.$$

Table 3. THE TIME DIFFERENCING SCHEMES.

Name	Scheme	Characteristics
Euler	$k^{(n+1)} = k^{(n)}+\Delta t f^{(n)}, f^{(n)} \equiv f(k^{(n)}, n\Delta t)$	Explicit,Truncation accuracy of $O(\Delta t)$
Backward	$k^{(n+1)} = k^{(n)}+\Delta t f^{(n+1)}$	Implicit, $O(\Delta t)$
Trapezoidal	$k^{(n+1)} = k^{(n)}+\frac{1}{2}\Delta t(f^{(n)}+f^{(n+1)})$	Implicit, $O[(\Delta t)^2]$
Matsuno	$k^{(n+1)^*} = k^{(n)}+\Delta t f^{(n)}$, $k^{(n+1)} = k^{(n)}+\Delta t f^{(n+1)^*}$, $f^{(n+1)^*} \equiv f(k^{(n+1)^*}, (n+1)\Delta t)$	Explicit, $O(\Delta t)$
Huen	$k^{(n+1)^*} = k^{(n)}+\Delta t f^{(n)}$, $k^{(n+1)} = k^{(n)}+\frac{1}{2}\Delta t(f^{(n)}+f^{(n+1)^*})$	Explicit, $O[(\Delta t)^2]$
Leapfrog	$k^{(n+1)} = k^{(n-1)}+2\Delta t f^{(n)}$	3 level, $O[(\Delta t)^2]$
Adams-Bashforth	$k^{(n+1)} = k^{(n)}+\Delta t(\frac{3}{2}f^{(n)}-f^{(n-1)})$	3 level, $O[(\Delta t)^2]$

For modeling this equation with a finite difference scheme, stability needs to be considered. The stability analysis was done using the von Neuman method. Except for Adams-Bashforth, all of the schemes in Table 3 were stable. The computer was used to chose the best one based on robustness with respect to the input parameters. A trial was made with a small time period and shallow mixed layer depth to test which scheme could handle the widest range of input parameters. The results suggested that the Huen scheme is the best for this problem, though it is only conditionally stable. The Huen scheme (in time), and the centered scheme, in space, was chosen for this problem:

$$\frac{\partial k}{\partial z} = \frac{k^n_{j+1}-k^n_{j-1}}{2\Delta z}$$

$$(\frac{\partial k}{\partial z})^2 = \frac{(k^n_{j+1}-k^n_{j-1})^2}{4(\Delta z)^2}$$

$$\frac{\partial^2 k}{\partial z^2} = \frac{k^n_{j+1}-2k^n_j+k^n_{j-1}}{\Delta z^2}$$

$$k_j^n = \frac{k_{j+1}^n + k_{j-1}^n}{2}$$

Therefore the finite difference form for step 1 of the Huen scheme is,

$$k_j^{(n+1)^*} = k_j^n + \Delta t \left[\frac{D}{8\Delta z^2} \left(\frac{k_{j+1}^n + k_{j-1}^n}{2} \right)^{-\frac{1}{2}} (k_{j+1}^n - k_{j-1}^n)^2 + \frac{D}{\Delta z^2} \left(\frac{k_{j+1}^n + k_{j-1}^n}{2} \right)^{\frac{1}{2}} (k_{j+1}^n - 2k_j^n + k_{j-1}^n) - \frac{1}{D} \left(\frac{k_{j+1}^n + k_{j-1}^n}{2} \right)^{\frac{3}{2}} \right] \tag{3}$$

and step 2 becomes,

$$k_j^{(n+1)} = k_j^n + \frac{\Delta t}{2} \left[\frac{D}{8\Delta z^2} \left\{ \left(\frac{k_{j+1}^n + k_{j-1}^n}{2} \right)^{-\frac{1}{2}} (k_{j+1}^n - k_{j-1}^n)^2 + \left(\frac{k_{j+1}^{(n+1)^*} + k_{j-1}^{(n+1)^*}}{2} \right)^{-\frac{1}{2}} (k_{j+1}^{(n+1)^*} - k_{j-1}^{(n+1)^*})^2 \right\} + \frac{D}{\Delta z^2} \left\{ \left(\frac{k_{j+1}^n + k_{j-1}^n}{2} \right)^{\frac{1}{2}} (k_{j+1}^n - 2k_j^n + k_{j-1}^n) + \left(\frac{k_{j+1}^{(n+1)^*} + k_{j-1}^{(n+1)^*}}{2} \right)^{\frac{1}{2}} (k_{j+1}^{(n+1)^*} - 2k_j^{(n+1)^*} + k_{j-1}^{(n+1)^*}) \right\} - \frac{1}{D} \left\{ \left(\frac{k_{j+1}^n + k_{j-1}^n}{2} \right)^{\frac{3}{2}} + \left(\frac{k_{j+1}^{(n+1)^*} + k_{j-1}^{(n+1)^*}}{2} \right)^{\frac{3}{2}} \right\} \right]$$

The grid system is chosen as shown in Fig. 6 because this is a one-dimensional problem.

2. Analytic Solution

The analytic solution for the steady state of this case can be derived. Equation (2) for steady state is

$$\frac{\partial}{\partial z} \left(v_t \frac{\partial k}{\partial z} \right) - \varepsilon = 0$$

where, $v_t = k^{\frac{1}{2}} D$, $\varepsilon = \frac{k^{\frac{3}{2}}}{D}$. Thus,

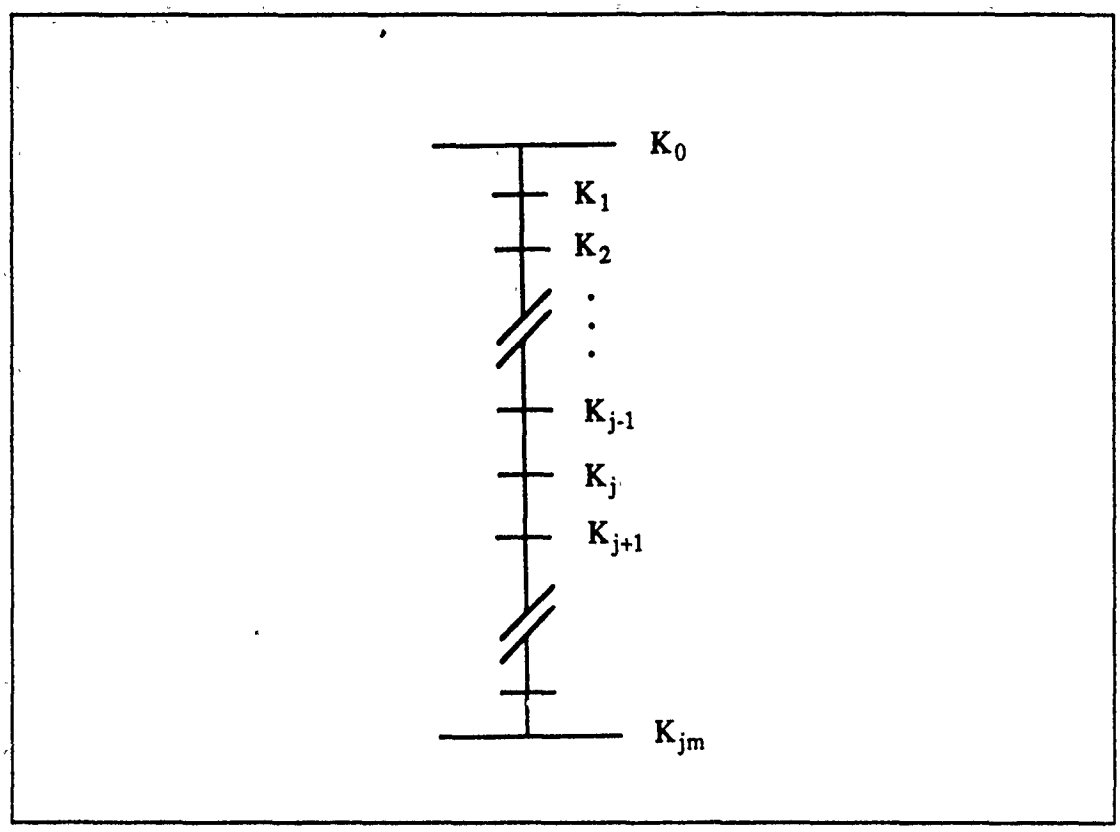

Figure 6. The Grid System for the Diffusion Model.

$$\frac{\partial}{\partial z}\left(k^{\frac{1}{2}} D \frac{\partial k}{\partial z}\right) - \frac{k^{\frac{3}{2}}}{D} = 0.$$

Let,

$$x_1 = k^{\frac{1}{2}} D \frac{\partial k}{\partial z}$$

$$x_2 = k^{\frac{3}{2}}$$

then a coupled linear system is,

$$x_1 = \frac{x_2}{D}$$

$$x_2 = \frac{3x_1}{2D}.$$

Solving this,

$$x_1 = ae^{\sqrt{\frac{3}{2}}\frac{z}{D}} + be^{-\sqrt{\frac{3}{2}}\frac{z}{D}}$$

$$x_2 = -\sqrt{\frac{3}{2}}\,ae^{\sqrt{\frac{3}{2}}\frac{z}{D}} + \sqrt{\frac{3}{2}}\,be^{-\sqrt{\frac{3}{2}}\frac{z}{D}}.$$

Since x_2 is finite at $z = +\infty$, a = 0. The solution is

$$k = k_0 e^{-\sqrt{\frac{2}{3}}\frac{z}{D}}$$

where $k_0 = (\sqrt{\frac{3}{2}}\,b)^{\frac{2}{3}} = k(z=0)$.

The analytic solution shows that the kinetic energy profile depends on the mixing length scale and the depth. With increasing depth, the kinetic energy is exponentially decaying. If the mixing length scale is larger, the kinetic energy decreases more slowly with depth. This solution was used to help verify that the diffusion model was working properly.

3. Stability Analysis

For the stability analysis, the von Neuman method was used. It is assumed that the solution will be of the form

$$k_j^n = R_e[k^n e^{lmj\Delta z}]. \tag{4}$$

Replacing the average terms $\left(\frac{k_{j-1}^n + k_{j-1}^n}{2}\right)$ in equation (3) by k_j^n, equation (3) becomes,

$$\begin{aligned}\frac{\partial k}{\partial z} = {} & \frac{D}{8\Delta z^2}(k_j^n)^{-\frac{1}{2}}\{(k_{j+1}^n)^2 - 2k_{j+1}^n k_{j-1}^n + (k_{j-1}^n)^2\} \\ & + \frac{D}{\Delta z^2}(k_j^n)^{\frac{1}{2}}(k_{j+1}^n - 2k_j^n + k_{j-1}^n) - \frac{1}{D}k_j^{n\frac{3}{2}}.\end{aligned} \tag{5}$$

Substitute (4) into (5), then

$$\begin{aligned}\frac{\partial k}{\partial z} = {} & \frac{D}{8\Delta z^2}(k_j^n)^{-\frac{1}{2}}\{(k^n)^2 e^{lk2(j+1)\Delta z} - 2(k^n)^2 e^{lk2j\Delta z} + (k^n)^2 e^{lk2(j-1)\Delta z}\} \\ & + \frac{D}{\Delta z^2}(k_j^n)^{\frac{1}{2}}(k^n e^{lk(j+1)\Delta z} - 2k^n e^{lkj\Delta z} + k^n e^{lk(j-1)\Delta z}) - \frac{1}{D}k_j^{n\frac{3}{2}}.\end{aligned} \tag{6}$$

This equation becomes,

$$\frac{\partial k}{\partial z} = (k_j^n)^{\frac{3}{2}} \left\{ \frac{D}{8\Delta z^2} (e^{2ik\Delta z} + e^{-2ik\Delta z} - 2) + \frac{D}{\Delta z^2} (e^{ik\Delta z} + e^{-ik\Delta z} - 2) - \frac{1}{D} \right\}. \tag{7}$$

Using the exponential relations with trigonometry, equation (7) becomes,

$$\frac{\partial k}{\partial z} = -(k_j^n)^{\frac{3}{2}} \{ \frac{D}{2\Delta z^2} (1 - \cos^2 ik\Delta z) + \frac{D}{\Delta z^2} (1 - \cos ik\Delta z) + \frac{1}{D} \}. \tag{8}$$

The expression inside the brackets is a constant, C, thus

$$\frac{\partial k}{\partial z} = -C(k_j^n)^{\frac{3}{2}}. \tag{9}$$

The first step of the Huen scheme is

$$\begin{aligned} k_j^{(n+1)^*} &= k_j^n + \Delta t f^n \\ &= k_j^n [1 - \Delta t C k_j^{n\frac{1}{2}}]. \end{aligned}$$

The second step is

$$\begin{aligned} k_j^{(n+1)} &= k_j^n + \frac{1}{2} \Delta t (f^n + f^{(n+1)^*}) \\ &= k_j^n [1 - \frac{1}{2} \Delta t C k^{n\frac{1}{2}} \{1 + (1 - \Delta t C (k^n)^{\frac{1}{2}})^{\frac{3}{2}}\}]. \end{aligned}$$

Let $A = \Delta t C k_j^{n\frac{1}{2}}$. The condition for stability is $0 \leq A \leq 1$. The A term is

$$(k_j^n)^{\frac{1}{2}} \{ \frac{\Delta t D}{2\Delta z^2} (1 - \cos^2 ik\Delta z) + \frac{\Delta t D}{\Delta z^2} (1 - \cos ik\Delta z) + \frac{\Delta t}{D} \} \leq 1. \tag{10}$$

If each term of equation (10), has equal weighing, then each term should be smaller than $\frac{1}{3}$. The first term,

$$\frac{1}{2} \frac{\Delta t D}{\Delta z^2} (k^n)^{\frac{1}{2}} \leq \frac{1}{3}$$

gives the condition for Δt,

$$\Delta t \leq \frac{2}{3} \frac{\Delta z^2}{D(k_j^n)^{\frac{1}{2}}}. \tag{11}$$

The second term,

$$\frac{\Delta t D}{\Delta z^2}(k^n)^{\frac{1}{2}} \le \frac{1}{3},$$

also gives a condition for Δt,

$$\Delta t \le \frac{1}{3}\frac{\Delta z^2}{D(k_j^n)^{\frac{1}{2}}}. \tag{12}$$

Similarly for the third term,

$$\frac{\Delta t}{D}(k^n)^{\frac{1}{2}} \le \frac{1}{3}.$$

$$\Delta t \le \frac{1}{3}\frac{D}{(k_j^n)^{\frac{1}{2}}}. \tag{13}$$

Condition (12) is smaller than (11) or (13) because the value of Δz is usually smaller than the value of D, therefore Δt should satisfy condition (12). In this criterion for stability of Δt, the TKE itself is included due to the non-linearity of the problem. The value for TKE changes depending on time and depth.

4. Initial Conditions

The diffusion model was initially tried for calm conditions. The initial kinetic energy everywhere within the whole grid was set to zero. A certain amount of kinetic energy flux was given at the very top grid point and allowed to diffuse downward. This trial failed due to the initial zero value of TKE, which appears in the denominator of equation (3). To avoid this problem, another trial was made which substituted the term which has k in the denominator with a separate variable. These trials looked successful but the stability criterion was more severe than the first trial forcing a limited range for D, the mixing length scale. Because of this limitation, this path was abandoned and instead a non-zero initial value for the TKE, k_0, in the turbulent layer was used. Eventually, the value used for k_0 came from the bulk model. The results of the diffusion model typically show a profile that decays exponentially initially with depth, but soon reaches an equilibrium and then maintains a constant amount of TKE to the bottom of the grid. Grid dependence is inappropriate and thus the MLD value from the bulk rain model needs be used as another input. Used in this fashion, this model was useful for predicting the fine structure within the mixed layer. Further refinement of this model might increase its usefulness (adding buoyancy, etc.).

C. THE NPS BULK MODEL

1. Review of the Wind Mixing Model

Garwood (1977) presented a bulk mixed layer model for the upper ocean mixed layer due to wind mixing and the buoyancy flux of heat and salinity. These forcing terms (wind mixing and buoyancy fluxes) have been the principle focus of upper ocean layer (homogeneous) modeling in recent decades. As an initial attempt to model a mixed layer forced by raindrop kinetic energy, the NPS bulk mixed layer model was adjusted term by term. Thus each term of the rain-induced NPS bulk mixed layer model will be interpreted based upon an understanding of the wind driven mixed layer model.

The depth of the wind-driven mixed layer depends on the balance between wind forcing, buoyancy damping, usually represented by surface heating, and the destabilization of the lower interface. The resulting entrainment is due to Kelvin-Helmholtz instabilities. The best conditions for mixed layer development and deepening are wind mixing while surface cooling is occurring. This combination is the main cause for latitudinal and seasonal mixed layer depth variations on large scales and for diurnal variations on small scales. The oceanic mixed layer is usually characterized by a uniform temperature layer, disregarding the effect of salinity. The atmospheric forcing terms (surface heat flux and wind shear) and the vertical velocity term (rate of shoaling or deepening of the mixed layer bottom) should be given.

The bulk mixed layer model uses a vertical integration of equation (1) across the turbulent mixed layer. The source term for wind mixing is the shear stress from wind (term (A) of equation (1)), and the intermittent upward surface buoyancy flux through the surface (term (B) of equation (1)). It is usually assumed that a shear zone exists at the top of the layer and that the thickness of shear zone, h_s, is much shorter than the mixed layer depth. There is assumed to be no shear zone at the base of the mixed layer.

In the entrainment zone, the flux Richardson number (R_F) is proportional to R_i (the bulk Richardson number). The flux Richardson number is defined as follows,

$$R_F = \frac{\alpha g \overline{T'w'}}{\overline{u'w'}\frac{\partial \bar{u}}{\partial z} + \overline{v'w'}\frac{\partial \bar{v}}{\partial z}}.$$

Thus term (A) from equation (1) can be written as

$$-\alpha g \frac{\overline{T'w'}}{R_F}.$$

The buoyancy term, derived from the equation of state for sea water, is

$$\tilde{\rho} = \rho_0[1-\alpha(T-T_0)+\beta(s-s_0)] \tag{14}$$

where $\tilde{\rho} = \rho_0+\rho'$, ρ_0, T_0, s_0 are the mean values of density, temperature and salinity, respectively, and α and β are the expansion coefficients. The definition for buoyancy is

$$\tilde{b} = \frac{\rho_0-\tilde{\rho}}{\rho_0} g. \tag{15}$$

By combining (14) and (15),

$$\tilde{b} = g(\alpha\Delta T-\beta\Delta s).$$

The surface buoyancy flux (B_0) for the vertically integrated model is

$$B_0 = \overline{b'w'}_0 = [\alpha g\overline{T'w'}_0-\beta g\overline{s'w'}_0]. \tag{16}$$

Ignoring the salinity effect because of the assumption that the salinity of both upper and lower layer is same (in wind mixing), the surface heat flux $\overline{T'w'}_0 = -Q$. Therefore

$$B_0 = -\alpha gQ$$

and the entrainment buoyancy flux (B_h) becomes

$$B_h = [\alpha g\overline{T'w'}_{-h}]$$

where $\overline{T'w'}_{-h}$ is the heat flux at the bottom of the mixed layer.

The entrainment buoyancy flux can be combined with the shear stress term into a single expression

$$-\left(\frac{1}{R_F}-1\right)\alpha g\overline{T'w'}. \tag{17}$$

Furthermore, an entrainment velocity, W_e, can be defined

$$W_e = \frac{\partial h}{\partial t}+\overline{w}_{-h}$$

where h is the MLD and $\overline{w}_{-h}$ represents mean vertical motion. The heat flux at the entrainment zone can be expressed as,

$$-\overline{Tw'}_{-h} = \Delta\overline{T}W_e \tag{18}$$

Thus, (17) becomes

$$\alpha g\Delta\overline{T}W_e(1-\frac{1}{R_F}).$$

The transport term, (C), represents the TKE transport from the surface to the entrainment zone. Some portion of the energy will dissipate and rest will work to deepen the MLD. This term can be expressed as the ratio of available TKE, $<\overline{E}>$, to the time scale, τ, required to transport the energy. The energy should be transported a distance of h (MLD). Therefore, the time scale (τ) is taken to be proportional to h divided by the rms vertical velocity scale, $<\overline{w'^2}>$:

$$\tau = a_1 h <\overline{w'^2}>^{-\frac{1}{2}}.$$

Term (C) becomes,

$$a_1 \frac{<\overline{E}><w'^2>^{\frac{1}{2}}}{h}. \tag{19}$$

The left hand side of equation (1), the unsteadiness term, $\frac{\partial E}{\partial t}(-h-\delta)$, can be expressed as $a_3\frac{<\overline{E}>W_e}{h}$.

Neglecting dissipation, equation (1) can now be written as follows in entrainment zone:

$$a_3\frac{<\overline{E}>W_e}{h} = -a_4\alpha g\Delta\overline{T}W_e + a_1\frac{\overline{<w'_{rms}{}^2>}^{\frac{1}{2}}<\overline{E}>}{h}.$$

Where a_1, a_3 and a_4 are tuning constants. If they are assumed to be order one as an initial guess, then the entrainment velocity can be expressed as:

$$W_e = \frac{(\overline{w'^2})^{\frac{1}{2}}<\overline{E}>}{[\alpha gh\Delta\overline{T}+\overline{E}]}. \tag{20}$$

Thus the model can be used to predict the deepening of the mixed layer.

The dissipation term is the most questionable quantity. The net viscous dissipation term was entirely neglected (Kraus and Turner 1967) or assumed to be proportional to the source term (Niiler 1975). But these models have a flaw of a continual increase in the potential energy of density stratification and a unlimited deepening of the mixed layer for no surface heat flux cases. The limiting value of the mixed layer depth appears to be proportional to the Monin-Obukhov length scale (L) in the Niiler model, while the real world situation it is better estimated using the Ekman scale. As a more advanced expression, Zilitinkevich et al. (1979) assumed the bulk dissipation to be

$$\int_0^h \varepsilon dz = (a_4 + a_5 \mid \mu_0 \mid) \frac{v_*^3 h}{\lambda},$$

where λ is the Ekman scale, v_* is friction velocity, β is the buoyancy parameter, f is the Coriolis parameter and μ_0 is the stratification parameter. This expression appears to be in better agreement with experimental data when compared with earlier models (Zilitinkevich et al. 1979).

The viscous dissipation of turbulent energy is governed by the cascade energy transfer from larger to smaller eddies, and occurs primarily at the length scale of the smallest eddies. Garwood (1977) made an estimate of dissipation by taking the rate at which the largest eddies supply energy to the smaller eddies to be proportional to the reciprocal of the time scale of the largest eddies. For shallow mixed layers, high Reynolds number ($R_* \gg 1$), an integral model for dissipation in the mixed layer, independent of viscosity and the small scale is

$$\int_{-h-\delta}^{0} \varepsilon dz = m_1 < \overline{E} >^{\frac{3}{2}}$$

where $\overline{E}$ is the vertical mean of turbulent energy and m_1 is a constant of proportionality, roughly equal to 1 for wind mixing. Thus, ε becomes

$$\varepsilon = \frac{m_1 < \overline{E} >^{\frac{3}{2}}}{h}.$$

In the case of deeper mixed layers ($R_* \sim 1$), the time scale is the inverse of the Coriolis parameter, and simplest combination of the two scales gives

$$\int_{-h-\delta}^{0} \varepsilon dz = m_1 < \overline{E} >^{\frac{3}{2}} + m_5 f h < \overline{E} > .$$

Therefore ε is

$$\varepsilon = m_1 \left[\frac{< \overline{E} >^{\frac{3}{2}} + f < \overline{E} >}{h} \right].$$

For the bulk mixed layer model, Garwood chose the shallow mixed layer case (Gaspar 1988).

2. Adapting the Bulk Model to Rain Induced Mixing

The wind mixing model needs to be adjusted to the case of rain induced mixing. For rain-induced mixing there is no mean shear, so term A from equation (1) is zero. The source term becomes the portion of term (C) that is evaluated at the surface after vertical integration. How much of the raindrop kinetic energy is available to act as a source of turbulence? When the rain drop hits the water surface, subsurface vortex rings, Rayleigh jets and surface gravity waves are created. Only subsurface vortex rings represent energy that goes to mixing. This fraction of energy, η , is an important tuning constant for the source term of the rain induced mixed layer model. The rest of the drop energy is presumably dissipated at the surface (although a tiny fraction, 10^{-6}, goes into sound energy). The source term has the form: $\eta \times \frac{1}{2} \rho I (WR)^2$, where WR is the raindrop terminal velocity.

There have been many investigations of raindrop terminal velocity. Beard and Prauppacher (1969) presented a summary of results of these investigations, and collected data which agreed quite closely with those of Gunn and Kinzer (1949). Even though there was a flaw of using drops which were allowed to fall in an environment of air of only 50% relative humidity, the study of Kinzer and Gunn has been regarded as the most complete and widely quoted in the literature. In this paper we use these data to assign terminal velocities to varying rain drop sizes. The drop sizes used by Green and Houk were 2.2 mm, 3.6 mm and 5.5 mm in diameter. The terminal velocities for these drop sizes are: 690 cm/s for a drop diameter of 2.2 mm, 860 cm/s for 3.6 mm drops and 915 cm/s for 5.5 mm drops (Gunn and Kinzer 1949).

One of the more different aspects of the rain mixing model compared with the wind mixing model is the fact that salinity is a major source of buoyancy damping. For

this reason, the oceanic mixed layer is defined as a uniform density layer rather than a uniform temperature layer. From Equation (16), the surface buoyancy working rate becomes

$$B_0 = -p[\alpha g(T_p - T) + \beta g s]h$$

where the surface heat flux is $\overline{T'w'}_0 = -p(T_p - T)$, the surface salinity flux is $\overline{s'w'}_0 = ps$, p is the precipitation rate multiplied by density and divided by 2, i.e. $\frac{1}{2}\rho I$, and I is rain intensity. The entrainment buoyancy flux becomes

$$B_h = W_e[\alpha g(T_b - T) + \beta g(s - s_b)]h.$$

Where, T_p is precipitation temperature, T_b is bottom temperature, s_b is bottom salinity, T and s are the instantaneous temperature and salinity of the mixed layer, and W_e is the entrainment velocity.

Keedy's experiments intimate the fact that the penetration of a rain drop is mainly a vertical process. This makes it possible to assume that the total TKE $E = \overline{u'^2} + \overline{v'^2} + \overline{w'^2} \simeq \overline{w'^2}$. When E is substituted by $\overline{w'^2}$ in equation (20), the entrainment velocity for rain mixing is

$$W_e = M_4 \frac{< \overline{E} >^{\frac{3}{2}}}{[\alpha g h \Delta \overline{T} + \overline{E}]} \tag{21}$$

where M_4 is a tuning constant.

As in the wind mixing model, identifying the dissipation term is difficult. For rain mixing, the Reynolds number (R_e) is the ratio of advection to viscosity, which can be expressed as $R_e = \frac{\sqrt{E}\, D}{\nu}$ where D is the length scale of stirring by individual rain drops. When the Reynolds number is large (unstable), the total dissipation is proportional to the total TKE, E, and the mixed layer depth, h, and is inversely proportional to the mixing length scale; i.e., $\int \varepsilon dz = M_1 \frac{\nu E}{D^2} h$. If R_e is small (stable), the dissipation term may be dominated the viscosity, so that $\int \varepsilon dz = \nu(\frac{E^{\frac{1}{2}}}{D})^2 h = \nu \frac{E}{D^2} h$. The dissipation term adapted for this model is a combination of these two cases; i.e.,

$$\int \varepsilon dz = M_1(\frac{\nu E}{D^2} h + \frac{E^{\frac{3}{2}}}{D} h). \tag{22}$$

M_1 is a tuning constant. For wind mixing it is order 1 but for rain mixing its magnitude is not known. Different values will be allowed in this study.

The Obukhov length scale for the ocean mixed layer depth can be represented as the ratio of source term to the surface buoyancy working rate. The precipitation rate cancels out when these two terms are set equal. The remaining terms can be expressed for the mixed layer depth (h) or for η ; i.e.,

$$B_0 = -p(\alpha g(T_p - T) + \beta g S)h =$$

$$Source = p\eta(WR)^2.$$

For h,

$$h = -\frac{\eta(WR)^2}{\alpha g(\Delta T) + \beta g S}.$$

For η,

$$\eta = -\frac{\alpha g \Delta T + \beta g S}{(WR)^2} h.$$

Therefore, when we know the mixed layer depth roughly, we can estimate η. This means that for the steady state, the mixed layer depth is not the function of rain rate, but only that of the source and surface buoyancy term. And when the surface buoyancy works as a production term (such as cold rain on warm water), the mixed layer depth can grow continuously.

3. Tuning constants

A summary of the tuning constants used in this model are as follows:

M_1: dissipation rate

M_4: Entrainment coefficient

D : Mixing length scale

η : The fraction of input energy which penetrates the surface boundary layer and works as a source term

One more possibility is the initial mixed layer depth h_0. This term could be used to represent the depth to which the raindrops penetrate during their initial impacts. The bulk model does not require that this be non-zero, however it was observed that non-

zero values produced model results closer to the experimental mixed layer depths. The values chosen for h_0 were arbitrary (order centimeters) or predicted from the bulk model itself by running the bulk model in a spin-up mode (very small time step) until the rate of change of TKE, $(\frac{\partial k}{\partial t})$, became small. The bulk model was then restarted with the h_0 from the spin-up mode and with a larger time step.

The dissipation term was composed in a reasonable manner, however there exists the possibility that it is proportional to the expression we developed. This possibility is allowed through the dissipation coefficient, M_1, which can be different from one (the value usually assumed as a first guess). Similarly, the entrainment term has a tuning constant coefficient, M_4, which is not necessarily unity. In the wind mixing model, these coefficients are both order one. In this rain model, we allowed both M_1 and M_4 to change as we expect that the mixing due to rain may occur on a tiny scale compared with wind mixing. The entrainment could be smaller, or the dissipation could be larger than with wind mixing.

The mixing length scale, which was assumed to be proportional to the rain drop size, effects the MLD but not very strongly. It was used as a fine tuning constant. The value for η is completely unknown because there are no prior studies which predict what portion of total energy may go into subsurface mixing.

The biggest obstacle for tuning this model was the fact that there is not enough experimental data to be used for tuning. Most of the data published by Green and Houk consists of only one data point after 40 minutes or two data points (10 min and 40 min) for a few chosen cases. This required us to assume values for several constants so that we could tune one of them and then retune the other constants in an interactive manner. M_1 and M_4 should be universal constants for the model given a mixing length scale (D) and η can be different in different situations.

4. Procedure for Verification

The NPS bulk rain model used the IBM package program 'IODE' which solves differential equations. Each term of equation (1) was made into a special function, constant or derivative so that closure was satisfied. Initially we assumed that the dissipation coefficient is one (M_1=1) and that all the rainfall kinetic energy goes directly into subsurface mixing (η = 1). The model was tuned to the experimental data using M_4 at first and then fine tuned by varying D. Varying M_4 strongly affected the mixed layer depth while varying D only produced minor changes.

The next trials were made by setting M_1 and M_4 equal to one, the values they normally assume in wind mixing models, and varying η and the initial mixing depth. These assumptions implied that the dissipation and entrainment velocity formulations are the same as in the wind mixing model, but that the fraction of raindrop kinetic energy working to create turbulence could be less than one. Tuning was done by fixing η so that the MLD after 10 minutes matched the experimental data and D had some reasonable value. The initial mixing depth was then adjusted to match the 40 minute data.

The last trials were made by varying M_1 and η at the same time with M_4 fixed at a value of one. The value of D was set proportional to drop size (10 times drop size). The initial mixing layer depth, h_0, was predicted from the model in a spin-up mode. In order to have the model estimate an initial value for h_0, the model was run with a very short time step (10^{-2} sec) until $\frac{\partial E}{\partial t}$ was small. The depth of mixed layer at this time was taken to be h_0. The model was restarted using a larger time step with h_0, the initial TKE and the time set to the value given by the spin-up model. By varying η and M_1, optimum values for η and M_1 pairs were identified.

IV. RESULTS AND DISCUSSION

In the following discussion, the results of each set of trials which were introduced in the previous chapter will be discussed. Even though my tuning effort is not a complete one, I tried to predict reasonable sets of tuning constants for salty water and fresh water. Additional experiments are needed for more precise tuning of this model.

The results of the first trials ($M_1 = 1, \eta = 1$) suggested that the mixing length scale (D) is proportional to drop size. Figure 7 shows the relation of D to drop size when M_4 is 0.003 in salty water. The different values of D for the same drop size are due to differences in rain intensity. This suggested a comparison of rain intensity versus mixing length scale. Figure 8 shows this comparison. For a given drop size, the value of D

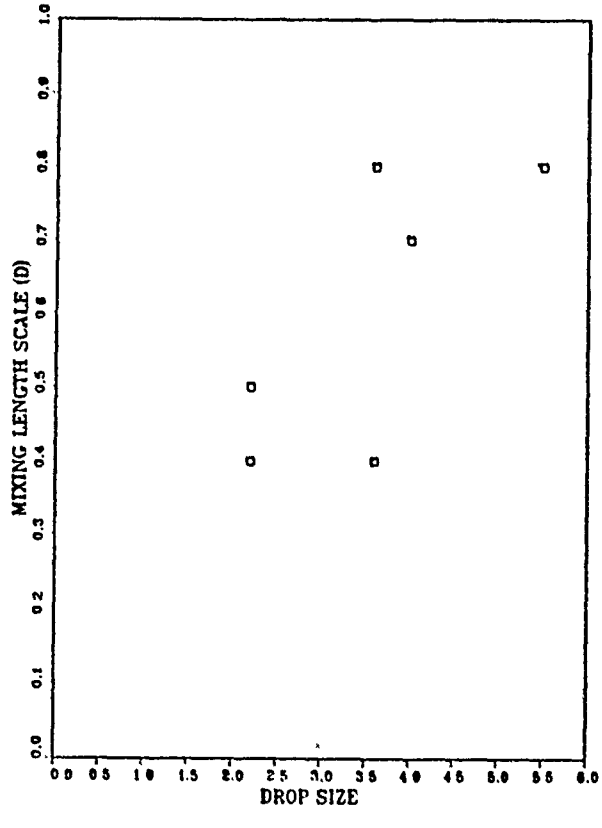

Figure 7. Mixing Length Scale (in cm) versus Drop Sizes (mm) in Salty Water. M_4 is 0.003, M_1 and η are equal to one.

is proportional to the rain intensity. The relationship has a different slope for each drop size. For larger drop sizes, the slope is much greater than for the smaller drop sizes. Thus, the mixing length scale is proportional to both drop size and rain intensity.

In the first trials, M_4 was set at 3×10^{-3} so that the mixed layer depth of the model fit that of the experiments. However, there is no physical reason why this entrainment coefficient should be much smaller than in the wind mixing case ($M_4 = 1$). For this reason, M_1 and M_4 were fixed in the second set of trials to a value of one and then η was varied. In order to roughly reproduce the experimental data, the value of η was of order 10^{-3}.

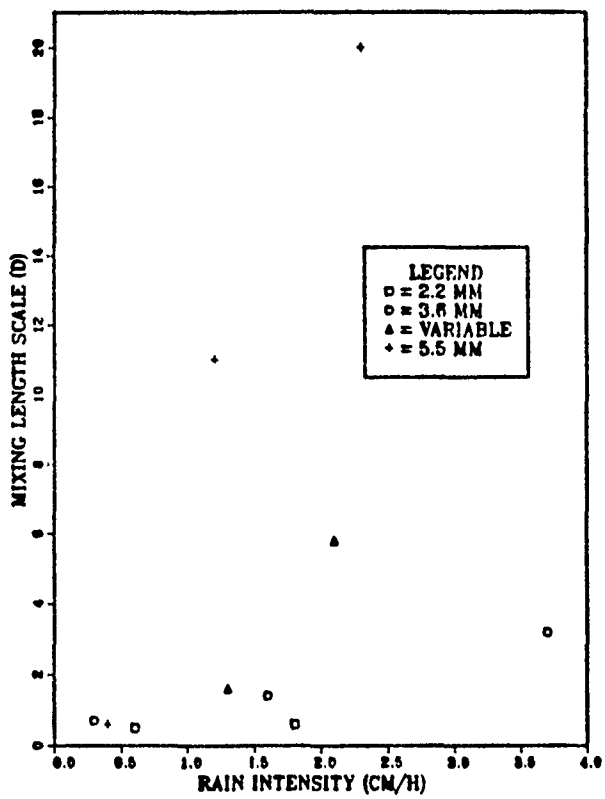

Figure 8. The Behavior of Mixing Length Scale versus Rainfall Intensity for Each Drop Size.

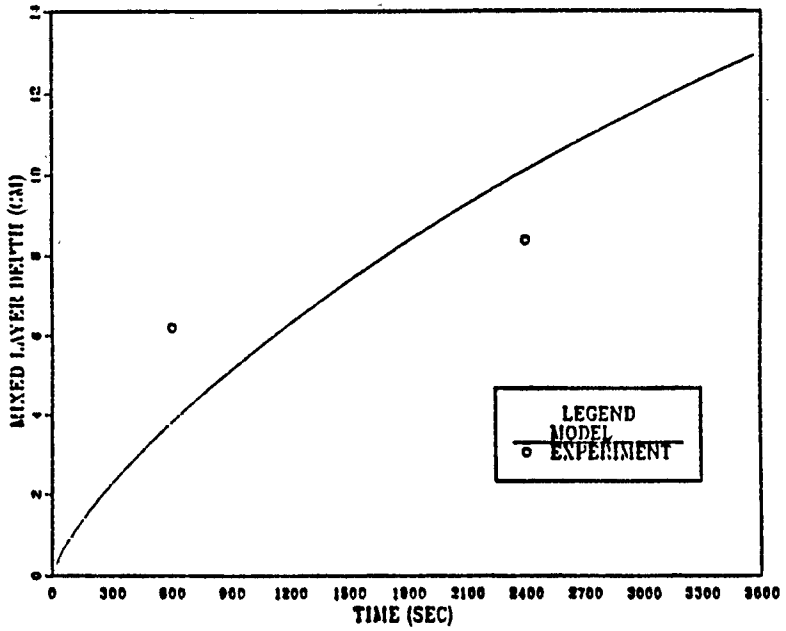

Figure 9. A Comparison of Model Prediction to Experimental Data. The drop size was 2.2 mm and the rain intensity was 0.6 cm/h. The experimental data is after 10 and 40 minutes rainfall.

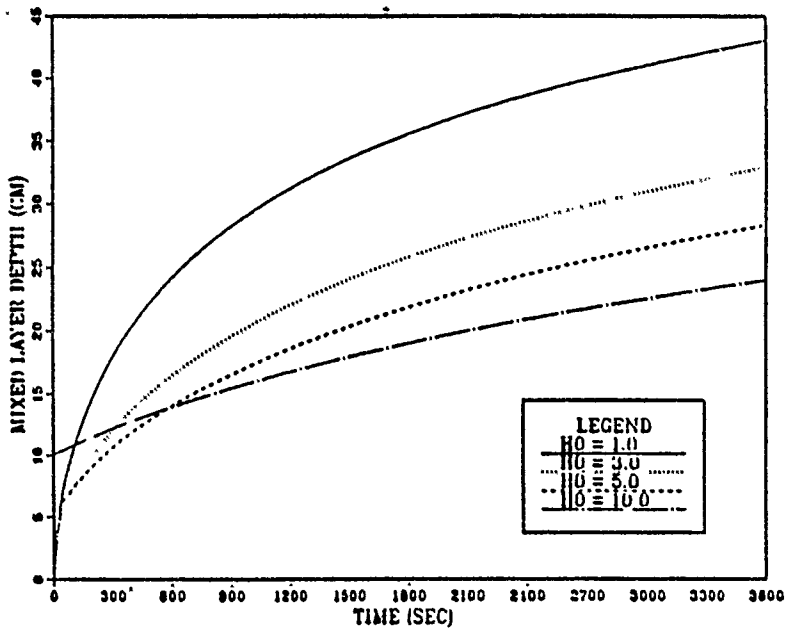

Figure 10. The Mixed Layer Depth Profile for Various Initial MLDs. For 3.6 mm drop size and 1.6 cm/h rain intensity. The initial mixed layer depth was chosen arbitrarily.

Green and Houk published their experimental data at 10 and 40 minutes only. When I adjusted the model to match to the mixed layer depth data at 40 minutes, the model at 10 minutes had a smaller mixed layer than that of the experiments, i.e., the model MLD value increases less rapidly than in the laboratory experiments. Figure 9 shows a typical case where the model is fitted to the experimental data so that the total error (rms difference) is minimized. This means that the mixed layer depth needs to arrive at an equilibrium depth earlier. This can be accomplished by changing the initial mixed layer depth, h_0 . The mixed layer depth for different initial mixed layer depths are represented in Figure 10. When the initial mixed layer depth is deeper, the MLD reached an equilibrium state sooner. This suggests the possibility of the existence of an

Table 4. MLD FOR EACH DROP SIZE when D and h_0 are tuned with the condition of $M_1 = M_4 = 1$, and $\eta = 0.002$. The DT and DH values are the experimental data after for 10 min./40 min. of rain onto fresh water.

Drop and Intensity	h_0 (cm)	D (cm)	h(model)	DT (cm)	DH (cm)
2206	5.0	0.7	6.0/8.2	5.7/7.2	6.2/8.4
2218	7.2	0.5	8.3/10.8	8.0/11.0	8.5/11.2
3603	5.0	0.5	6.1/8.4	5.0/7.8	7.7/10.2
3616	7.0	0.7	10.3/15.7	10.5/14.8	11.7/16.7
3637	8.5	2.0	15.3/25.7	15.3/25.0	15.3/24.7
5504	3.5	0.4	5.7/9.3	5.5/8.9	5.7/9.8
5512	4.0	3.0	13.0/24.6	13.5/27.0	13.9/27.5
5523	20.0	12.0	25.4/37.3	28.0/38.5	25.6/37.4
V13	8.5	1.3	11.1/16.5	10.1/16.2	11.3/16.7
V21	15.0	8.0	18.7/27.1	19.7/26.0	18.8/25.5

initial mixed layer depth (h_0). This initial mixed layer depth can be interpreted as the rain drop penetration depth caused by the initial physical impact. Following this suggestion, trials were made to examine the behavior of the initial mixed layer depth and D.

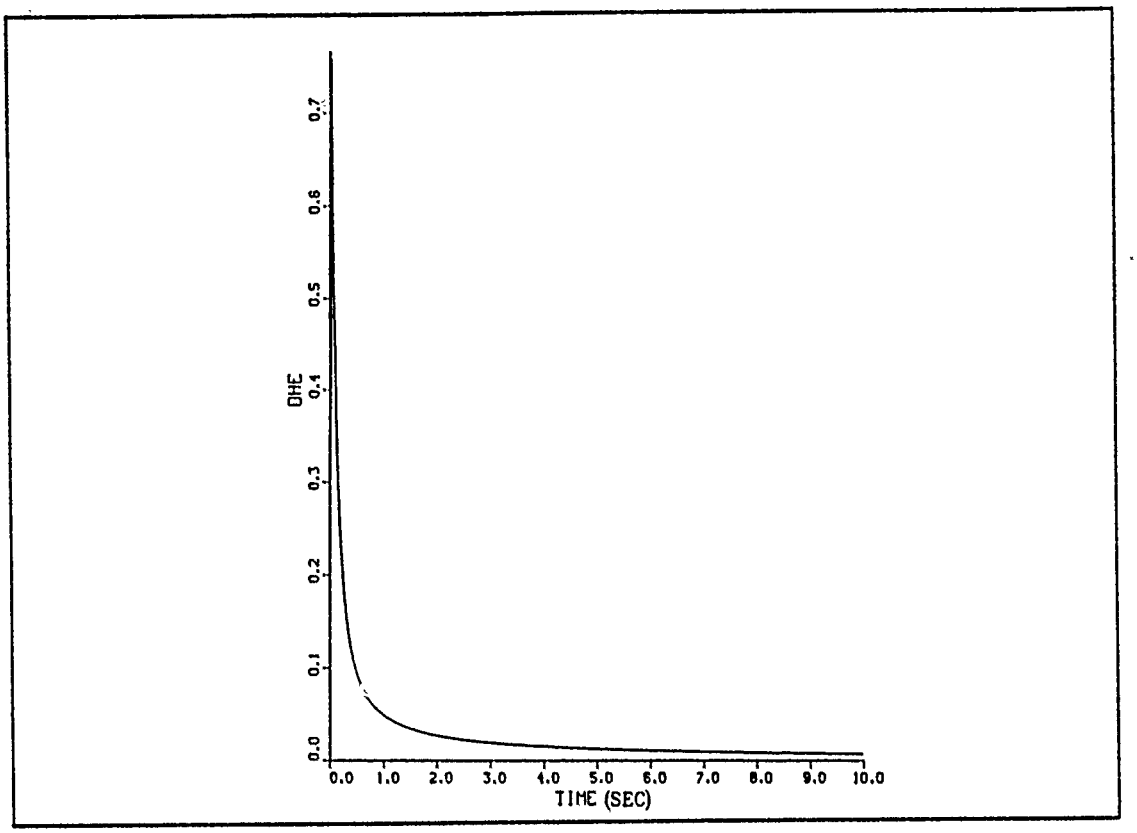

Figure 11. The Spin-up Mode Criterion for Rate of Change of TKE. Usually the criterion was order of 10^{-2}.

Table 4 shows the results for the case of $M_1 = M_4 = 1$, and $\eta = 0.002$. The first two digits in the first column indicate the drop sizes (in mm) and the second two digits indicate rain intensity in cm/h without decimal point between each two number. For example, 3616 means 3.6 mm diameter drops at a rainfall intensity of 1.6 cm/h. This notation will be used through out this paper. V indicates variable drop sizes in the rain. DT and DH are the mixed layer depth data from Green and Houk where DT is the mixed layer depth defined as the depth of maximum temperature gradient, while DH is the mixed layer depth defined as the depth at which 90% of the heat transferred through the surface is stored. The mixed layer depths from the model and the experiments are recorded after 10 minutes and 40 minutes of rainfall. The initial mixing depth looks roughly proportional to the drop size and rain intensity. Even though this definition for

the initial mixing depth is quite attractive, it introduces an additional free tuning constant, h_0 , which requires additional assumptions.

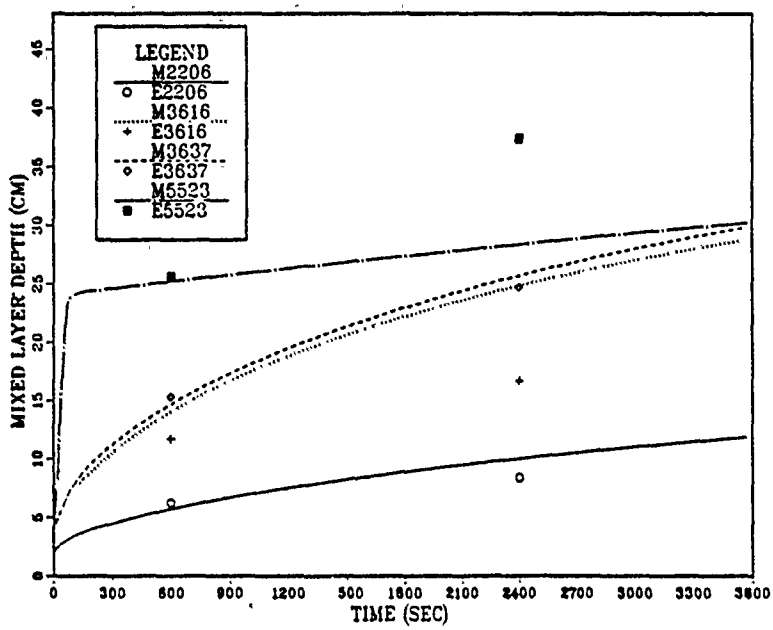

Figure 12. The Mixed Layer Depth Profile for Chosen Drop Sizes. The number 5523 means 5.5 mm drop diameter and 2.3 cm/h rain intensity. The continuous data is the model data and the point data is the experimental data after 10 and 40 minutes rainfall.

As mentioned earlier, the model does not necessarily need h_0 to be treated as a free tuning constant. Garwood suggested a spin-up mode for the rain model. In order to have the model estimate an initial mixed layer depth, h_0 , the model was run with a very short time step (10^{-2} sec) until $\frac{\partial E}{\partial t}$ was small enough. The criterion for small enough was on the order of 10^{-2}. For example, Figure 11 shows the behavior of the change of TKE ($\frac{\partial E}{\partial t}$) with time. Another run was then started with a larger time step using the initial time, h_0, and HE, the total turbulent kinetic energy, from the spin-up mode. Using the initial depth value from the spin-up mode, MLD profiles are presented in Figure 12 for different drop sizes and compared to the experimental data.

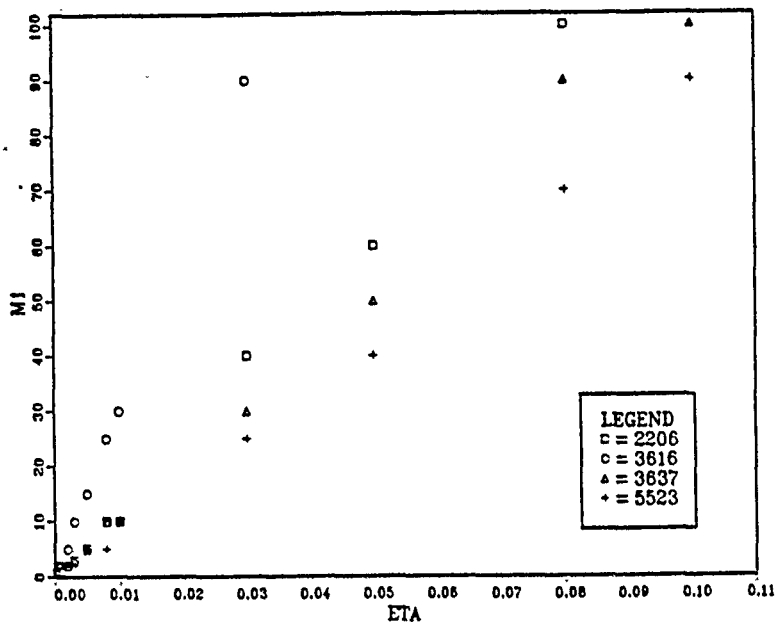

Figure 13. The Optimum Value (Least Error Square) of M_1 and η for chosen drop sizes.

The last tuning trials focused on the values for η and M_1 . The dissipation coefficient, M_1, can be one as in the wind mixing model, but might have another value. The value of M_4 was fixed to one and the value of D was chosen to be 10 times rain drop diameter. The value of η was varied from 10^{-4} to 10^{-1} while the value of M_1 was varied from 1 to 100. For each set of η and M_1, the mixed layer depth after 10 minutes and 40 minutes data was compared with that of the experiments. Figure 13 shows the optimum pair of M_1 and η for each selected drop size. The optimum pair was defined as the M_1 and η pair which has the minimum least square error when compared to the experimental MLD after 10 and 40 minutes. As M_1 is believed to be a universal constant, these results suggest that η is proportional to drop size and rain intensity. Table 5 shows the combined (summation over all drop sizes) least square error for each pair of M_1 and η from Fig. 3. A band of optimal M_1 and η pairs is apparent.

We don't expect the value of M_1 to be much larger than that of the wind mixing case ($M_1 = 1$). Therefore, η is probably less than 0.01 implying that the TKE used in subsurface mixing is less than 1% of the total kinetic energy of the rain. If the dissipation rate is very large ($M_1 \sim 100$), then η may be as high as 10%.

Table 5. COMBINED LEAST SQUARE ERROR FOR EACH M_1 AND η PAIR.

M_1 / η	0.001	0.002	0.003	0.005	0.008	0.01	0.03	0.05	0.08
1	162.5	551.5	1177.8	2630.9					
2		163.3							
5	712.9	302.4	174.8	164.3	388.5	604.7			
10			422.1	214.6	141.8	162.9	1221.4		
15			621.7	366.1	195.8	151.0	611.6		
20				502.6	288.1	211.0	361.5	936.0	
25					379.1	286.9	241.9	619.6	
30						360.7	204.2	430.1	
40							178.5	239	
50							187.4	162.2	
60							241.3	139.7	
70								141.6	201.5
80								157.0	162.8
90								182.3	144.2
100								208.4	138.2

To demonstrate combining the diffusion model with the bulk model, a pair of η and M_1 from Table 5 was chosen for further analysis. While this pair ($\eta = 0.08$, $M_1 = 100$) had the minimum combined least square error in Table 5, these values for η and M_1 may not be the true values for these constants. Nevertheless, the bulk rain model was run

with these constants for 20 minutes of rainfall. After 20 minutes of rainfall, the mixed layer depth and total TKE from the bulk model were recorded and used as the initial conditions for the diffusion model. Figure 14 presents the TKE profile from the diffusion model for four different rainfall conditions. The results suggest that rain containing larger drop sizes generates deeper mixed layer depths and more turbulent mixing.

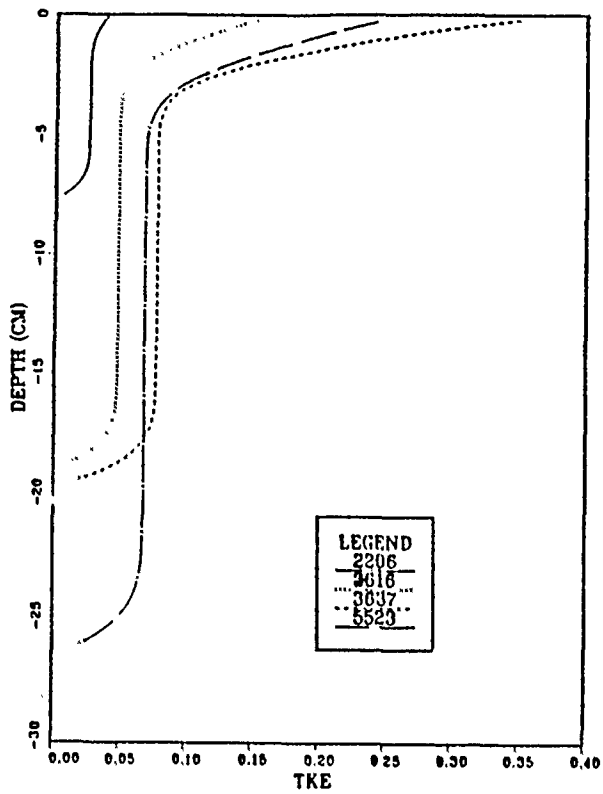

Figure 14. The TKE Profile from the Diffusion Model. For chosen drop sizes in fresh water. The depth is in cm. The notation 2206 means that the raindrop size is 2.2 mm and the rain intensity is 0.6 cm/h. The other numbers have similar interpretation.

The Richardson number reflects stability. The entrainment velocities were studied with respect to this number in the experiments of Green and Houk. Their results show that the entrainment velocity is proportional to the reciprocal (slope is -1) of the Richardson number. That the entrainment velocity is bigger in the unstable state than in the stable state appears to be a common phenomena. The NPS bulk rain model was investigated for this relationship.

in the stable state appears to be a common phenomena. The NPS bulk rain model was investigated for this relationship.

The rain Richardson number was defined by Garwood. For the upper layer,

$$R_i \equiv \frac{h(\alpha g \Delta T + \beta g s)}{(WR)^2.}$$

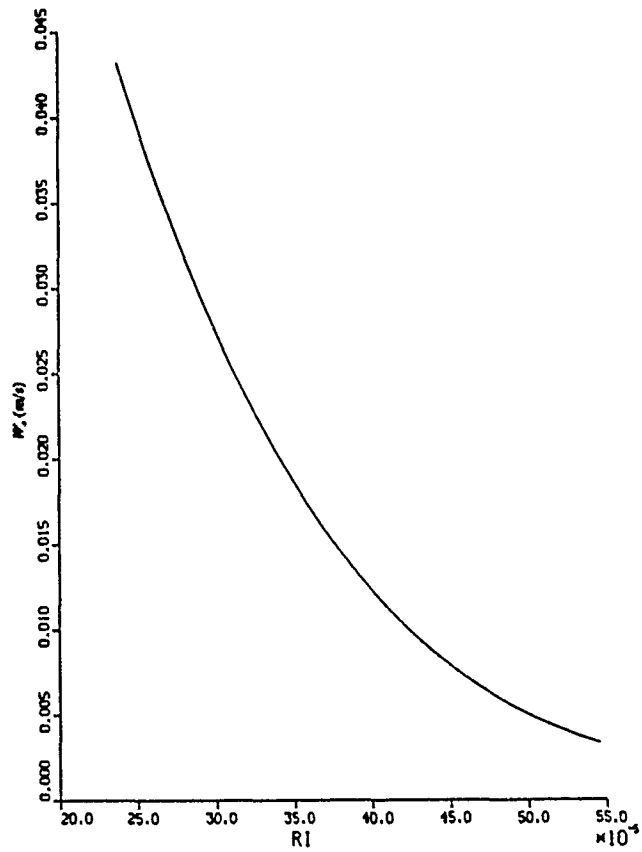

Figure 15. The Richardson Number Versus Entrainment Velocity

For the rain model, the relation between entrainment velocity (WE) and the Richardson number is presented in Figure 15. This result shows that the entrainment velocity is roughly proportional to the reciprocal of the Richardson number for the bulk rain model.

The most helpful function of a model may be prediction. With this in mind, I chose a M_1, η pair from the previous trial (M_1=100, η=0.08). We assume a hypothetical rain with a uniform raindrop size of roughly 3.6 mm and an intensity of 1.6 cm/h in the

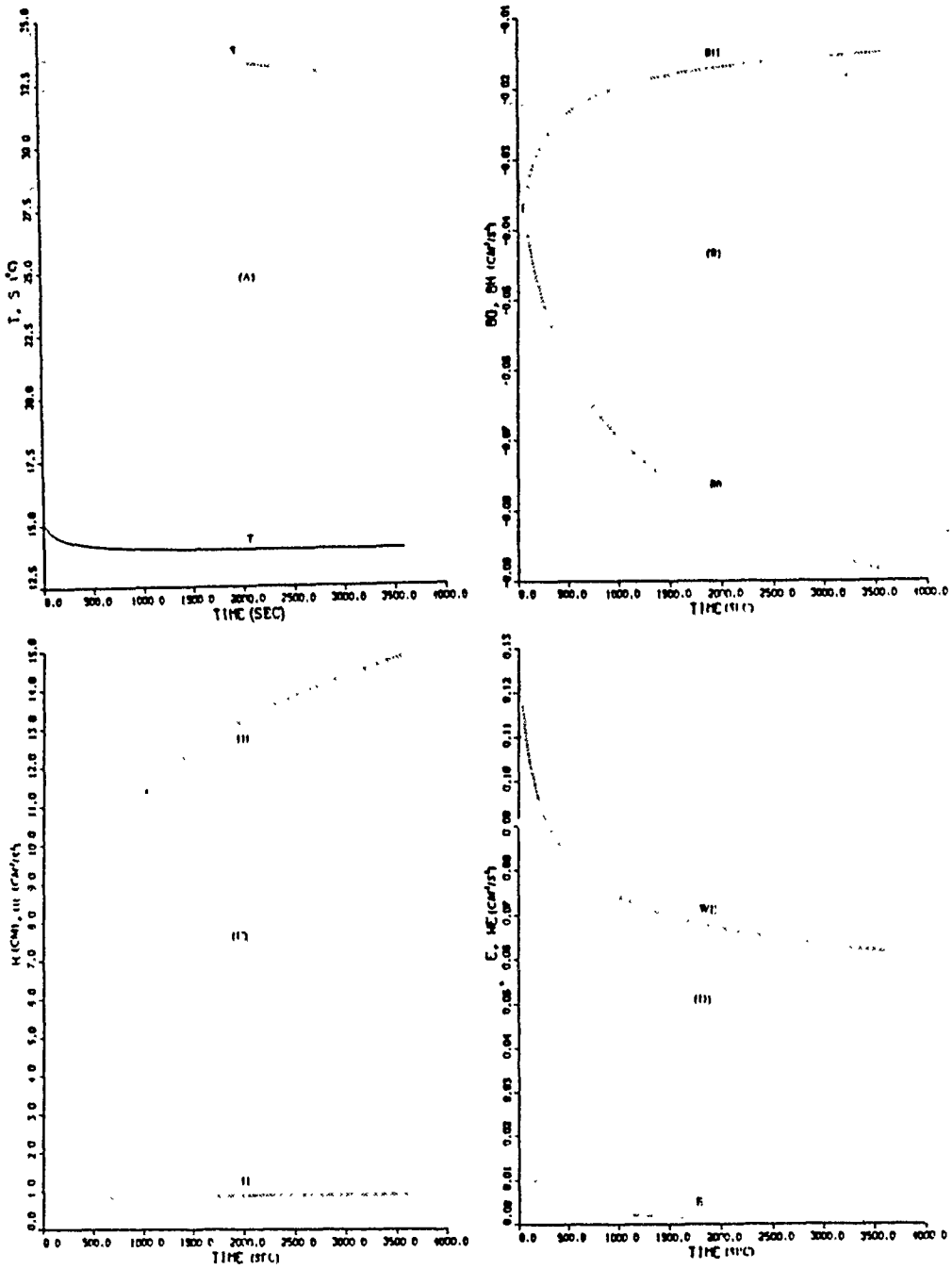

Figure 16. The Time History of Each Parameter in the Rain Bulk Model: (A) is for temperature (T) and salinity (S), (B) is for buoyancy working rate at the surface (B0) and at the bottom of MLD (BH), (C) is for mixed layer depth (H) and total TKE (HE) and (D) is for the TKE (E) and entrainment velocity(WE).

is chosen to be 34.4 ppt, an average value at mid-latitudes in the north Pacific (Pickard and Emery 1982). The spin up time was chosen to be 15 seconds. After this spin up time, the initial mixed layer depth was 5.4 cm. Figure 16 shows the time history for each parameter in the bulk model. As the figure shows, the salinity within the mixed layer, S, decreases continuously with time due to dilution. The temperature, T, quickly reaches an equilibrium state and maintains that level. The buoyancy flux at the surface, B0, decays with time due to the mixing. The buoyancy flux at the bottom of entrainment zone, BH, increases rapidly initially, but then slowly increases. The entrainment velocity, WE, decreases with time and the average kinetic energy, E, also decays with time. However, the total kinetic energy, HE, increases because the mixed layer depth is increasing continually.

Finally, after 5, 15, 30 and 60 minutes of rain, values for MLD and TKE were recorded and used as inputs for the diffusion model. The mixed layer TKE profiles from the diffusion model are shown in Fig. 17.

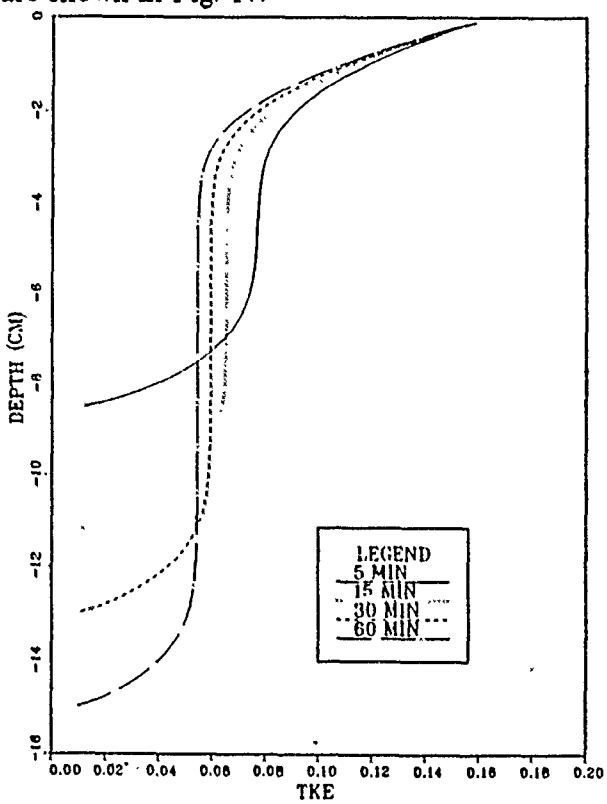

Figure 17. The TKE Profile For Hypothetical Rain Conditions in the North Pacific.

V. CONCLUSIONS AND RECOMMENDATIONS

There is clear evidence that rainfall generates a thin turbulent mixed layer at the ocean surface. Such a mixed layer will effect air-sea interaction processes, however the strength and character of that turbulent layer is unknown.

This paper has attempted to model the formation of the rain-induced turbulent layer by modifying the existing NPS wind mixing bulk model to the situation of rain mixing. The resulting NPS rain mixing bulk model has several tuning constants associated with it: η, the percent of the raindrop kinetic energy available for mixing; M_1,the dissipation rate; M_4 , the entrainment rate; D, the mixing scale and, perhaps , h_0, the initial penetration depth of the rain drops. By examining the values that these tuning constants were required to assume to have the model match experimental data, we can draw some conclusions about the rain-induced mixed layer.

For the NPS wind mixing model, the dissipation rate and entrainment rate constants are order one (i.e. $M_1 = M_4 = 1$). If the rain model also assumes that they are order one, then η is order 10^{-2}. This implies that only 1% of the kinetic energy of the raindrops will go into subsurface mixing. The rest of the energy stays at the surface in the form of ripples or surface waves. Alternatively M_4 may be small (order 10^{-3}), which seems physically unsatisfactory, or M_1 can be larger (order $10 \sim 100$). In fact, given a value for M_1, η has an optimum value which may be proportional to drop size and rain intensity. However, with $M_1 = 100$, η is still only 0.08. Therefore the conclusion that very little of the raindrop kinetic energy is available for subsurface mixing seems very solid.

Another conclusion is that the mixing length scale is proportional to both drop size and rainfall intensity. There is also some indication that there is an initial penetration depth which is order of centimeters and also proportional to both drop size and rainfall intensity.

An attempt was made to model the rain induced mixed layer with a diffusion model. In this study the diffusion model took a trivial role of providing internal fine structure given initial conditions from the NPS rain mixing bulk model. There is possibility of further development for this model; in particular, the addition of the buoyancy terms should be attempted.

Finally a prediction for the formation of a rain-induced mixed layer is provided given some hypothetical rain conditions in the North Pacific Ocean.

The experimental data used to constrain the model consisted of two mixed layer depths (after 10 and 40 minutes) for a variety of artificial laboratory rainfall situations. This was not sufficient to fix the values of the tuning constants used in the model. Further experimental data should remedy this problem. In particular it should be possible to design laboratory experimental procedures to identify η, the energy available for mixing; D, the mixing length scale; h_0, the initial penetration depth of the raindrops and M_4, the entrainment rate. To monitor the formation of the mixed layer, the data should be recorded continuously, rather than at just two discrete time points.

APPENDIX A. THE NPS BULK RAIN INDUCED MIXED LAYER MODEL

```
VARIABLES & INITIAL CONDITIONS:
HE = .0
H = .1000000000D-01
S = 34.40000000
T = 20.00000000
TIME = .0

CONSTANTS:
AG = .2000000000
BG = .8000000000
SB = 34.40000000
TP = 18.00000000
TB = 19.00000000
M1 = 100.0000000
M4 = 1.000000000
D = 3.600000000
NU = .1000000000D-01
WR = 860.0000000
P = .5000000000D-03
EBS = .8000000000D-01

SPECIAL FUNCTIONS:
E = HE/H
WE = M4*E*SQRT(E)/(E+H*(AG*(T-TB)+BG*(SB-S)))
BO = -P*(AG*(TP-T)+BG*S)*H
BH = WE*H*(AG*(TB-T)+BG*(S-SB))
DIS = -2.*M1*(NU*HE/D**2+E*SQRT(E)*H/D)
DHE = SOURCE+BO+BH+DIS
SOURCE = EBS*P*WR**2

DERIVATIVES:
D(HE /D(TIME ) = =
    SOURCE+BH+BO+DIS
D(H /D(TIME ) = =
    WE+P
D(S /D(TIME ) = =
    (WE*(SB-S)-P*S)/H
D(T /D(TIME ) = =
    (WE*(TB-T)+P*(TP-T))/H

OUTPUTS:
   TITLE: RAIN MIXING
   TABULATE: TIME    H       HE      E       WE      DHE     SOURCE  DIS

      AT INTERVAL    .1000000000D-01
   PLOT: H       HE      DHE     DIS
      AGAINST: TIME   AT INTERVAL    1.000000000

END CALCULATION WHEN TIME .GE. 30.0000
```

APPENDIX B. CODE OF THE DIFFUSION MODEL

```
*****************************************************************
*                                                               *
*          TURBULENT KINETIC ENERGY DIFFUSION MODEL             *
*                                                               *
*****************************************************************
*                                                               *
*      THIS MODEL DEALT THE DIFFUSION OF TKE WITH THE GIVEN     *
*   INITIAL TKE VALUE AND MIXED LAYER DEPTH. THE UNIT OF MI-    *
*   XED LAYER DEPTH IS CM, AND OF RAIN INTENSITY IS CM/H.       *
*                                                               *
* ************************************************************* *
*                                                               *
*   TKE  : VARIABLE WHICH IS REPRESENTING THE TURBULENT KIN-    *
*          ETIC ENERGY (TKE).                                   *
*   TKEO : VARIABLE WHICH IS REPRESENTING THE TKE VALUE OF      *
*          ONE TIME STEP BEFORE.                                *
*   TKEN : VARIABLE WHICH IS REPRESENTING THE TKE VALUE OF      *
*          ONE TIME STEP AFTER.                                 *
*   TKE0 : THE VALUE OF TKE EXIST INITIALLY.                    *
*   TKET : THE VALUE OF TOTAL TKE AT A GIVEN TIME. GIVEN BY     *
*          USER.                                                *
*   DT   : TIME STEP.                                           *
*   DZ   : SPACE STEP.                                          *
*   RHO  : DENSITY OF WATER IN CGS UNIT (= 1.0).                *
*   WR   : THE TERMINAL VELOCITY OF RAIN DROP.                  *
*   RR   : THE VALUE RAIN RATE. THE UNIT IS CM/H.               *
*   D    : MIXING LENGTH SCALE IN CM.                           *
*   ETA  : THE PORTION OF INPUT ENERGY WHICH IS USED FOR        *
*          SUBSURFACE MIXING AS A SOURCE TERM.                  *
*   DEP  : DENSITY OF WATER IN CGS UNIT (= 1.0).                *
*   P    : SPACE STEP WHICH USER WANT TO PRINT OUT.             *
*                                                               *
*****************************************************************
c
c Define the maximum time and space value.
c
      PARAMETER(JM=1000,JMP1=1000,NPTS=1000)
c
c Define variables.
c
      REAL*8 TKEO(0:JMP1),TKEN(0:JMP1),TKE(JM)
      REAL*8 DT,DZ,WR,RHO,RR,D,ETA,DEP,P,TKE0,TKET
c
      COMMON JMAXP
c
c Prepare the output data file.
c
      CALL EXCMS('FILEDEF 1 DISK THESIS DATA A')
c
c Read in data of mixed layer depth, total tke, mixing length scale,
```

```
c rain rate, and raindrop terminal velocity.
c
      PRINT*, 'WHAT IS THE VALUE OF MIXED LAYER DEPTH?'
      READ(5,*) JMAX
      PRINT*, 'WHAT IS THE VALUE OF TURBULENT KINETIC ENERGY AT THE
     1         SURFACE?'
      READ(5,*) TKET
      PRINT*, 'WHAT IS THE VALUE OF MIXING LENGTH SCALE?'
      READ(5,*) D
      PRINT*, 'WHAT IS THE VALUE OF RAIN DROP TERMINAL VELOCITY?'
      READ(5,*) WR
      PRINT*, 'WHAT IS THE RAIN INTENSITY?'
      READ(5,*) RR
c
c Set the values of constants.
c
      JMAXP = JMAX + 1
      DT = 0.1D-02
      DZ = 0.1D00
      RHO= 1.0D00
      ETA= 1.0D-03
      P  = RR*RHO/(7.2D+03)
      TKE0 = P*WR**2
c
c  Set the initial condition.
c
      DO 11 J=1,JMAX
       TKE(J) = 0.0
11    CONTINUE
c
c  Set the value at time=0
c
      DO 22 J=1,JMAX
       TKE0(J) = TKET
22    CONTINUE
c
c Set the boundary condition using the subroutine 'BNDRY'.
c
      CALL BNDRY(TKE0,ETA)
c
c Main loop (time loop)
c
      DO 100 N=1,NPTS
c                             set the boundary conditions.
         CALL BNDRY(TKEN,ETA)
c                             compute Tke using huen scheme.
         CALL HUEN(TKE0,TKEN,DT,DZ,D,NPTS,JMAX,JMAXP)
c                             tansfer the tke for next time loop.
         DO 55 I=1,JMAX
            TKE0(I) = TKEN(I)
            TKE(I)  = TKE0(I)
55       CONTINUE
c                             print out the results to data file using
c                             format.
         IF (MOD(N,1000).EQ.0) THEN
C           WRITE(1,*) 'SEC=',N/1000
```

```
            DO 777 J=1,JMAX/3
            DEP = -3*J*DZ
            WRITE(1,222) DEP,TKE(3*J)
777         CONTINUE
         END IF
222      FORMAT(' ',6D12.3)
100   CONTINUE
999   STOP
      END


*******************************************
*                                         *
*           Subroutine BNDRY              *
*                                         *
*******************************************
c
      SUBROUTINE BNDRY(KO,ETA)
c
      REAL*8 KO(0:JMAXP)
      REAL*8 ETA
c
      COMMON JMAXP
c
      KO(0) = ETA*KO
      KO(JMAX+1) = 0.0
c
      RETURN
      END


*******************************************
*                                         *
*           Subroutine HUEN               *
*                                         *
*******************************************
c
      SUBROUTINE HUEN(KO,KN,DT,DZ,D,NPTS,JM)
c
      REAL*8 KO(0:JMAXP),KN(0:JMAXP),DT,DZ,D,ETA
      INTEGER JMAXP
c
      COMMON JMAXP
C
c  Huen scheme
      DO 33 J=1,JM
         KN(J) = KO(J)+D*DT*(KO(J+1)-KO(J-1))**2/
     1         (8.*SQRT((KO(J+1)+KO(J-1))/2.D00)*DZ**2)
     2         + D*DT*SQRT((KO(J+1)+KO(J-1))/2.D00)*
     3           (KO(J+1)-2.*KO(J)+KO(J-1))/DZ**2 -
     4           DT*SQRT(((KO(J+1)+KO(J-1))/2.D00)**3)/D
33    CONTINUE
c
      DO 99 J=1,JM
          KN(J) = KO(J) + (DT/(16.*DZ**2))*(D*((KN(J+1)-
     5      KN(J-1))**2/SQRT((KN(J+1)+KN(J-1))/2.D00)
```

```
     6       + (KO(J+1)-KO(J-1))**2/SQRT((KO(J+1)+KO(J-1))/2.D00))
     7       + 8.D00*D*(SQRT((KN(J+1)+KN(J-1))/2.D00)*(KN(J+1)
     8       - 2.*KN(J)+KN(J-1))+SQRT((KO(J+1)+KO(J-1))/2.D00)
     9        *(KO(J+1)-2.D00*KO(J)+KO(J-1))) - 8.*DZ**2*
     A       (SQRT(((KN(J+1)+KN(J-1))/2.D00)**3)+KO(J)*SQRT(((KO(J+1)
     B        +KO(J-1))/2.D00)**3)))
C             WRITE(6,*) 'J=',J,'K(J)=',KN(J)
99    CONTINUE
c
      RETURN
      END
```

APPENDIX C. FLOW CHART FOR THE DIFFUSION MODEL

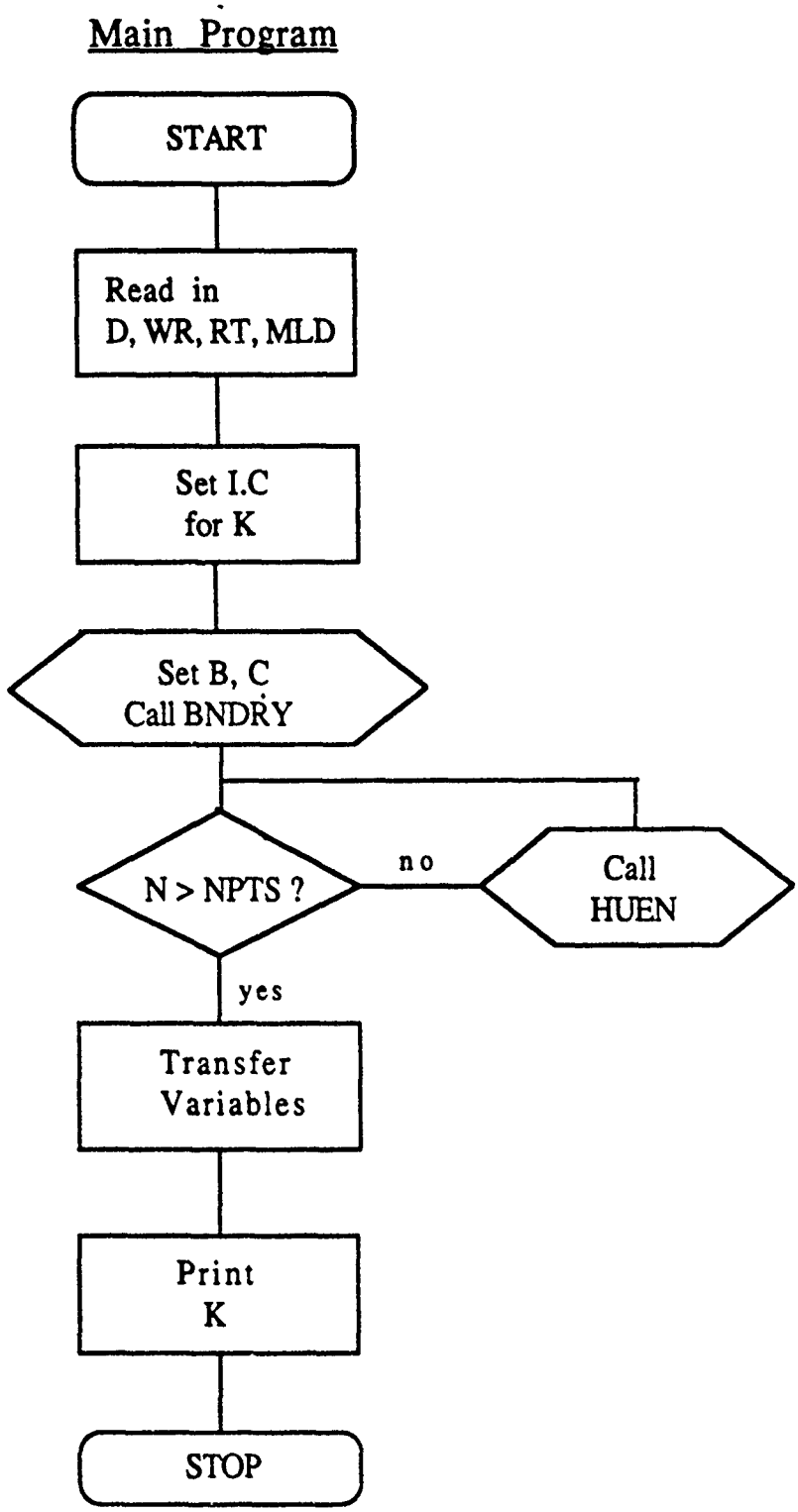

APPENDIX D. FLOW CHART FOR THE DIFFUSION MODEL (SUBROUTINE)

Subroutine HUEN

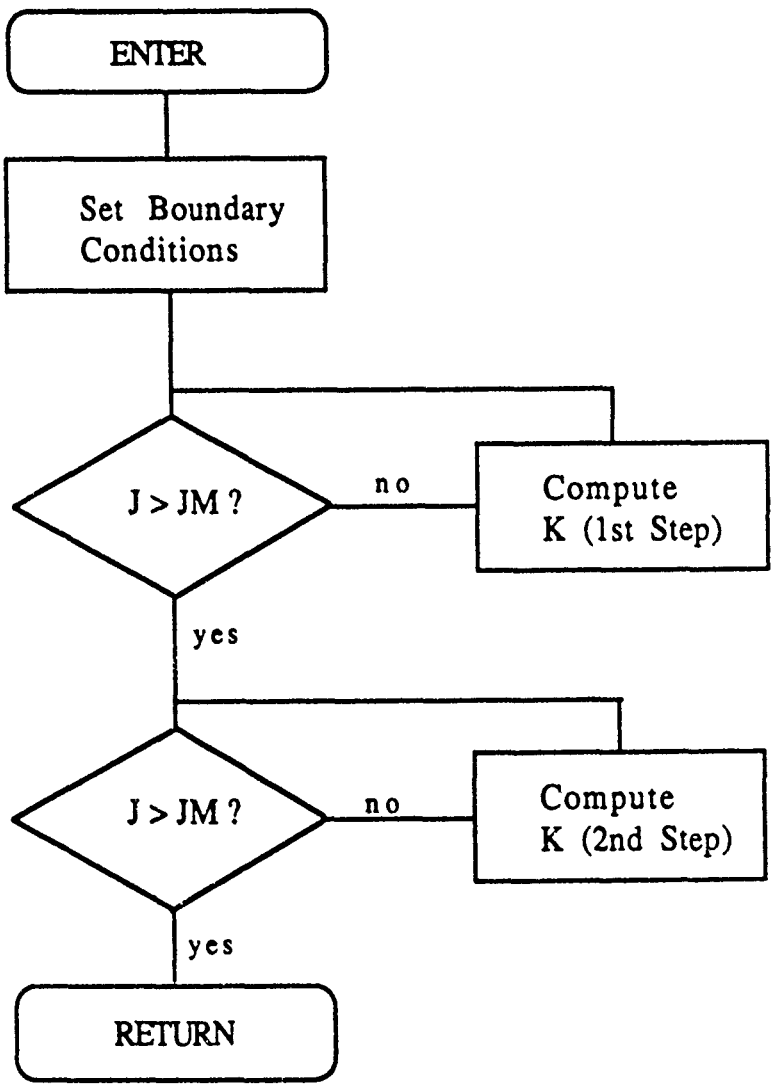

LIST OF REFERENCES

Beard, K. V. and Pruppacher, H. R., 1969: A determination of the terminal velocity and drag of small water drops by means of a wind turnnel, *J. Atmos. Scien.*, **26**, 1066 - 1072.

Chapman, D. S. and Critchlow, P. R., 1967: Formation of vortex rings from falling drops, *J. Fluid. Mech.*, **29**, 1, 177 - 185.

Garwood, R. W., 1977: An Ocean Mixed Layer Model Capable of Simulating Cyclic States, *J. Phys. Oceanogr.*,, **7**, 455 - 468.

Garwood, W. R., 1990: Personal communication.

Gaspar, P., 1988: Modeling the Seasonal Cycle of the Upper Ocean, *J. Phys. Oceanogr.*, **18**, 161 - 180.

Green, T. and Houk, D. F., 1979: The mixing of rain with near-surface water, *J. Fluid Mech.*, 90, 3, 569 - 588.

Gunn, R. and Kinzer, G. D., 1949: The terminal velocity of fall for water droplets in stagnant air, *J. Meteo.*, Aug., 243 - 248.

Keedy, H. F., 1967: Vortex rings formed by free surface interaction, Ph.D. Dissertation, The University of MIchigan, 141.

Kraus, E. B. and Turner, J. S.: A one-dimensional model of the seasonal thermocline, *Tellus XIX*, 1, 88 - 105.

Nystuen, J. A., 1990: A note on the attenuation of surface gravity waves by rainfall, *submitted to J. Geophys. Res.*.

Nystuen, J. A., 1990: Personal Communication.

Marshall, J. S. and Palmer, W. Mc., 1948: The distribution of rain drops with size, *J. Meteo.*, **5**, 165 - 166.

Pickard, G. L. and Emery, W. J., 1982: Descriptive physical oceanography an introduction, 4th edit., Pergamon, 195 - 208.

Poon, Y. K., Tany, S. and Wu, J., 1989: Rain generated ripples, *Abstract, AGU Fall Meeting, EOS Trans., Amer. Geophys. Union*, 70, 1168.

Siscoe, G. L. and Levin, Z., 1971: Water-drop-surface-wave intercation, *J. Geophy. Res.*, 76, 5112 - 5116.

Zilitinkevich, S. S., Chalikov, D. V. and Resnyansky, Yu. D., 1979: Modelling the oceanic upper layer, *Oceanol. Acta*, **2** , 2, 219 - 240.

INITIAL DISTRIBUTION LIST

		No. Copies
1.	Defense Technical Information Center Cameron Station Alexandria, VA 22304-6145	2
2.	Library, Code 0142 Naval Postgraduate School Monterey, CA 93943-5002	2
3.	Chairman (Code OC/Co) Department of Oceanography Naval Postgraduate School Monterey, CA 93943-5000	1
4.	Chairman (Code MR/Rd) Department of Meteorology Naval Postgraduate School Monterey, CA 93943-5000	1
5.	Jeffrey A. Nystuen (Code OC/Ny) Naval Post Graduate School Monterey, CA 93943-5000	3
6.	Roland W. Garwood (Code OC/Gd) Naval Post Graduate School Monterey, CA 93943-5000	1
7.	Kim Jong Rok SMC#2529 Naval Post Graduate School Monterey, CA 93943-5000	1
8.	Director Naval Oceanography Division Naval Observatory 34th and Massachusetts Avenue NW Washington, DC 20390	1
9.	Commander Naval Oceanography Command Stennis Space CTR, MS 39529-5000	1
10.	Commanding Officer Naval Oceanographic Office Stennis Space CTR, MS 39522-5001	1
11.	Commanding Officer Fleet Numerical Oceanography Center Monterey, CA 93943-5005	1

12. Commanding Officer 1
Naval Ocean Research and Development
Activity
Stennis Space CTR, MS 39529-5004

13. Commanding Officer 1
Naval Director Oceanographic &
Atmospheric Research Laboratory
Monterey, CA 93943-5006

14. Chairman, Oceanography Department 1
U. S. Naval Academy
Annapolis, MD 21402

15. Chief of Naval Research 1
800N. Quincy Street
Arlington, VA 22217

16. Office of Naval Research (Code 420) 1
Naval Ocean Research and Development
Activity
800N. Quincy Street
Arlington, VA 22217

17. Scientific Liaison Office 1
Office of Naval Research
Scripps Institution of Oceanography
La Jolla, CA 92037

18. Library 1
Scripps Institution of Oceanography
P. O. Box 2367
La Jolla, CA 92037

19. Library 1
Department of Oceanography
University of Wshington
Seattle, WA 98105

20. Library 1
CICESE
P. O. Box 4803
San Ysidro, CA 92073

21. Library 1
School of Oceanography
Oregon State University
Corvallis, OR 97331

22. Commander 1
Oceanographic Systems Pacific
Box 1390
Pearl Harbor, HI 96860

23. Library
R. O. K. Naval Academy
P. O. Box 100
Kyungnam Jinhaesi Anggokdong
Seoul, Korea — 1

24. Hur, Hong Beom
Choongbuk Okcheongun Okcheoneb
MoonjeongRi 6-2
Seoul, Korea — 5

25. Lee Kyung Taek
SMC#2990 Naval Post Graduate School
Monterey, CA 93943-5000 — 1